

## Acknowledgements

*I really want to thank my supervisor Ulf Lennart Osterberg for his great supporting all the time. I would also want to thank my partners at the laboratory, Hans, Lisa and Nils for their help during the experiments at lab and their friendliness.*

*I don't want to forget the great support with the software used offered by William Clench, from Newport company*

# Contents

<b>1</b>	<b>Introduction</b>	<b>1</b>
<b>2</b>	<b>Basis and Foundations</b>	<b>4</b>
2.1	Parameters of interest of Electromagnetic waves . . . . .	4
2.2	Properties of Ultrashort Laser Pulses . . . . .	6
2.2.1	The Intensity and Phase vs. Time and Frequency . . . . .	7
2.2.2	Phase distortions in Time and Frequency . . . . .	8
2.2.3	The Pulse Length and Spectral Width . . . . .	11
2.3	Nonlinear Optics . . . . .	11
2.4	Non-linear optical effects . . . . .	13
2.5	Time-frequency domain . . . . .	14
2.5.1	Short-Time Fourier Transform . . . . .	14
2.5.2	Time-Frequency localization . . . . .	15
2.5.3	The Spectrogram . . . . .	16
2.5.4	Wigner Transform . . . . .	19
2.6	WVD Drawbacks and conclusions . . . . .	22
<b>3</b>	<b>Previous alternatives techniques of measuring</b>	<b>23</b>
3.1	The Spectrum . . . . .	23
3.2	The Intensity Autocorrelation . . . . .	26
3.3	Combination of Autocorrelation and Spectrum . . . . .	30
<b>4</b>	<b>Frequency-Resolved Optical-Gating (FROG)</b>	<b>31</b>
4.1	Introduction and principal features . . . . .	31
4.2	Properties and advantages of FROG . . . . .	35
4.3	Impairments . . . . .	36
<b>5</b>	<b>FROG Device Setup</b>	<b>37</b>
5.1	The Ti:Sapphire laser . . . . .	37
5.2	Second-Harmonic-Generation FROG . . . . .	37
5.2.1	FROG Beam Geometries . . . . .	37
5.2.2	SHG FROG . . . . .	38
5.3	Setting-up SHG FROG Device . . . . .	40

<b>6</b>	<b>Measurements and analysis of FROG traces</b>	<b>51</b>
6.1	Newport FROG Software . . . . .	51
6.2	Femtosoft FROG 3.2.0. Software . . . . .	52
6.3	Characterization of our pulse of reference . . . . .	54
6.4	Increasing chirp effect . . . . .	61
6.4.1	10 <i>mm</i> Water cuvette . . . . .	61
6.4.2	50 <i>mm</i> Water cuvette . . . . .	64
6.4.3	100 <i>mm</i> Water cuvette . . . . .	66
<b>7</b>	<b>Conclusion</b>	<b>70</b>
7.1	Future work . . . . .	72
<b>8</b>	<b>Summary</b>	<b>73</b>
8.1	Experimental work . . . . .	76

# List of Figures

2.1	Temporal relationship between spectral components of a chirped pulse [18]	9
2.2	Chirped Pulse	10
2.3	Linear optics [6]	12
2.4	Nonlinear optics [6]	13
2.5	Second-harmonic generation	14
2.6	Types of windows used for STFT	14
2.7	Heisenberg box	15
2.8	Spectrogram with great resolution	17
2.9	Spectrogram with bad resolution	17
2.10	Couple of added signals in time 1	18
2.11	Couple of added signals in time 2	19
3.1	Michelson's interferometer [6]	24
3.2	Example of $sech^2$ pulse	26
3.3	Intensity Autocorrelator [6]	27
3.4	Autocorrelation [6]	28
4.1	Description of the spectrogram	32
4.2	FROG signal	33
4.3	Schematic of a generic FROG algorithm[15]	34
4.4	Spectrograms for Linearly Chirped Pulses [6]	35
5.1	Different FROG geometries. The prism/lens represents a spectrometer[6]	38
5.2	Difference between SHG and PG traces [6]	39
5.3	SHG FROG experimental setup [6]	40
5.4	SHG FROG Schematic of Newport [18]	41
5.5	Previous Routing Beam	43
5.6	Quantity of light that goes through the beamsplitter	44
5.7	The dispersive properties of Fused Silica [18]	45
5.8	Polarizing Cube	46
5.9	SHG FROG Device	47

5.10	SHG FROG Device . . . . .	48
5.11	SHG FROG Device . . . . .	49
5.12	SHG FROG Device . . . . .	50
6.1	Screenshot of FROG software of Newport . . . . .	52
6.2	Screenshot of FROG software Femtosoft . . . . .	53
6.3	Set up to measure the pulse of reference . . . . .	54
6.4	FROG trace of the reference pulse . . . . .	55
6.5	Original Pulse (a)(b) and Retrieved pulse (c)(d) . . . . .	56
6.6	Retrieved electric field from the reference pulse in (a) time domain and (b) frequency domain . . . . .	57
6.7	Comparison of FROG beam geometries . . . . .	58
6.8	Autocorrelation of the reference pulse . . . . .	59
6.9	Set up including a water cuvette of 10 <i>mm</i> . . . . .	61
6.10	FROG trace with 10 mm water cuvette . . . . .	61
6.11	Retrieved electric field from the reference pulse in (a) time domain and (b) frequency domain . . . . .	62
6.12	Original Pulse (a)(b) and Retrieved pulse (c)(d) . . . . .	62
6.13	Autocorrelation of the reference pulse . . . . .	63
6.14	Set up including a water cuvette of 50 <i>mm</i> . . . . .	64
6.15	FROG trace with a 50 mm cuvette included . . . . .	64
6.16	Retrieved electric field with a 50 mm cuvette included in (a) time domain and (b) frequency domain . . . . .	65
6.17	Original Pulse (a)(b) and Retrieved pulse (c)(d) . . . . .	65
6.18	Autocorrelation with a 50 mm cuvette included . . . . .	66
6.19	Set up including a water cuvette of 100 <i>mm</i> . . . . .	66
6.20	FROG trace with a 100 mm cuvette included . . . . .	67
6.21	Retrieved electric field a 100 mm cuvette included in (a) time domain and (b) frequency domain . . . . .	67
6.22	Original Pulse (a)(b) and Retrieved pulse (c)(d) . . . . .	68
6.23	Autocorrelation a 100 mm cuvette included . . . . .	68
6.24	Comparison of the spectral phases . . . . .	69
6.25	Comparison of the autocorrelations . . . . .	69
7.1	Evolution of the chirp effect using different water cuvette lengths . .	71
8.1	SHG FROG Device . . . . .	76
8.2	. . . . .	77
8.3	Newport FROG software Rev. 3 . . . . .	I
8.4	Femtosoft FROG 3.2.0 software . . . . .	III
8.5	Raw Data . . . . .	IV
8.6	Noise Subtraction . . . . .	V
8.7	Data . . . . .	V
8.8	Algorithm running . . . . .	VI

# Chapter 1

## Introduction

Nowadays, telecommunications and information technologies dominate the world. Advances in these areas have changed the people life's way around the world, what has led our current society to become the *Information Society*.

Much have evolved the telecommunications world and the way to transmit information throughout the years. Specially interesting have been the development of the optical communications since the discovery in 1958 of the *laser* (*Light Amplification by Stimulated Emission of Radiation*).

Transmitting light through optical fiber has permitted an amazing increase of the capacity of sending information, improving the quality of transmitted signal and increasing the velocities of transmission respect to the microwave communications through radio links and coaxial wires.

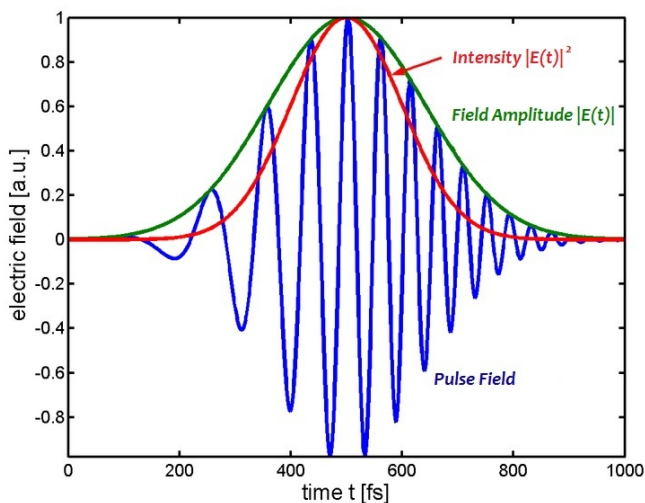
Furthermore, the laser has provided an quite important tool in order to measure any kind of fast event, the ultrashort light pulse (about a few femtoseconds ( $1fs = 10^{-15}$ )). And from this point we are going to focus on the measuring of fast events with ultrashort laser pulses, since many events occurs at these scales of time: key processes in biology like photosynthesis, key processes in chemistry (molecular vibrations) and key events in physics and engineering (photo-ionization and electron-hole relaxation times that determine the response times of light detectors and electronics)[1].

As well known, in order to measure an event in time we must use a shorter one, but then, to measure that shorter event, we need an even shorter one. And so on, until arriving at the shortest event ever created, the ultrashort pulse that has been said above.

In order to measure any fast event with an ultrashort laser pulse we need to check

that such pulse is in fact, a shorter event than the event we want to measure. Therefore, we must to measure our ultrashort laser pulse. If we study with detail the features of the pulse, we will obtain some key information about the possibilities and applications in which the ultrashort pulses can be very useful.

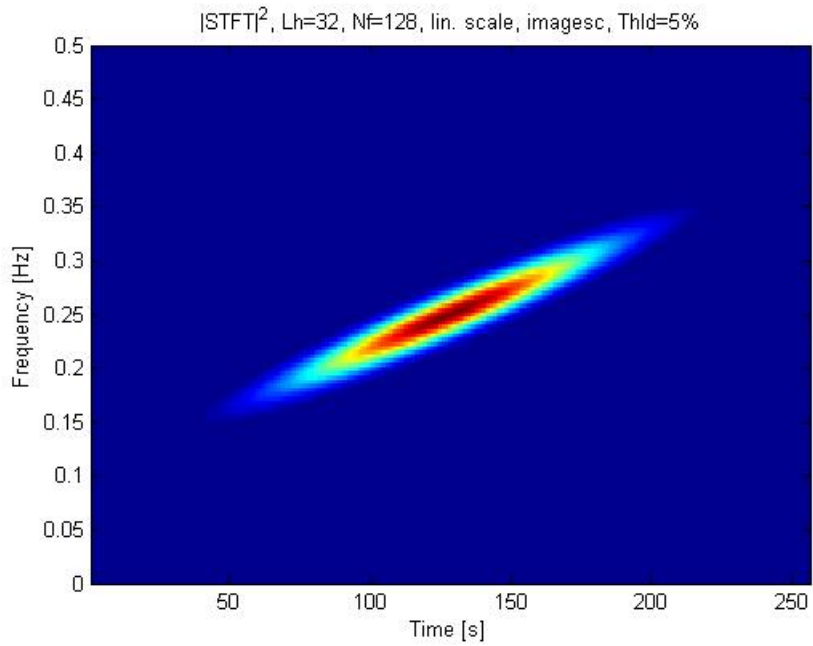
In the following chapter we will deal with the basis and foundations that we must take in account for the studying and measuring of the ultrashort pulses. We will describe in that chapter the ultrashort laser pulses and we will also define just what it is that we need to measure, it will be their intensity and phase. When we deal with ultrashort pulses we must to talk about the nonlinear optics, since linear optics cannot describe all the properties about the ultrashort pulses and its propagation.



We will also see in that chapter the great benefits of using the time-frequency domain for measuring the ultrashort pulses by the Frequency-Resolved Optical Gating technique, better known as FROG, its acronym. We will go through its advantages respect in both time domain and frequency domain separately.

In Chapter 3 we will see the techniques that preceded to the use of FROG for measuring ultrashort pulses which could not characterize the pulses completely, just the intensity. They are techniques as the intensity autocorrelation and the measuring of the spectrum.

In following chapters we will describe the FROG technique, as well as some assemblies done at the laboratory to check experimentally, from some measurements, the goodnesses of the FROG and comparing it with the autocorrelator performance.



Much has been written about FROG since in 1991 Rick Trebino and Daniel J.Kane invented it. Currently, a lot of laboratories around the world are working to improve the different FROG techniques and doing a hard research on it, in order to discover new applications in a width range of differents areas. In this thesis we will just deal with a small part of the whole possibilities that FROG can provide us.

# Chapter 2

## Basis and Foundations

### 2.1 Parameters of interest of Electromagnetic waves

As well known the electromagnetic waves propagation is well defined by the Maxwell's Equations, there are available some great papers that you can find and check at the bibliography of this thesis for a deeper research about the properties and features of such equations [2-3].

Starting with the four Maxwell Equations (in differential form)

$$\nabla \times \mathbf{H} = \mathbf{J} + \frac{\partial \mathbf{D}}{\partial t} \quad (2.1)$$

$$\nabla \times \mathbf{E} = -\frac{\partial \mathbf{B}}{\partial t} \quad (2.2)$$

$$\nabla \cdot \mathbf{D} = \rho_V \quad (2.3)$$

$$\nabla \cdot \mathbf{B} = 0 \quad (2.4)$$

and the so-called constitutive equations

$$\mathbf{D} = \epsilon \mathbf{E} \quad (2.5)$$

$$\mathbf{B} = \mu \mathbf{H} \quad (2.6)$$

$$\mathbf{J} = \sigma \mathbf{E} \quad (2.7)$$

it is possible to obtain the Telegrapher's Equation (here for the electric field  $\mathbf{E}$ ) by a few fundamental transformations [4]:

$$\nabla \times \nabla \times \mathbf{E} + \mu\sigma \frac{\partial \mathbf{E}}{\partial t} + \mu\epsilon \frac{\partial^2 \mathbf{E}}{\partial t^2} = 0 . \quad (2.8)$$

For the wave propagation in free space one can set  $\sigma = 0$  and the charge density  $\nabla \cdot \mathbf{D} = 0$  as well and obtain the wave equation

$$\Delta \mathbf{E} = \mu\epsilon \frac{\partial^2 \mathbf{E}}{\partial t^2} . \quad (2.9)$$

In general, the electric permittivity  $\epsilon$  and the magnetic permeability  $\mu$  can be described as the product of a relative, material dependent factor and the constant for the free space:

$$\mu\epsilon = \mu_r \mu_0 \epsilon_r \epsilon_0 \quad (2.10)$$

So let us start to talk about the part of interest that the electromagnetic wave has for us. From the Maxwell's Equations we obtain the Telegrapher's equation for the electric field  $\vec{E}$  and for the magnetic field  $\vec{B}$  respectively. After some assumptions, like the free space propagation, and taking the harmonic solution for the electric field  $\vec{E}$  we have:

$$\vec{E}(\vec{r}, t) = \Re[\mathbf{E}_0 * e^{j\vec{k}\vec{r} - j\omega t}] \quad (2.11)$$

where  $\vec{r}$  is the position vector and  $\vec{k}$  is the wave vector

$$\vec{k} = k * \vec{e}_k = (\omega \sqrt{\mu \epsilon(\omega)}) \vec{e}_k \quad (2.12)$$

where the permittivity is a function of  $\omega$ ,  $\epsilon(\omega) = \epsilon_r(\omega)\epsilon_0$ . So the wave vector is also a function of  $\omega$

$$\vec{k}(\omega) = \omega \sqrt{\mu_0 \epsilon_0} \sqrt{\epsilon(\omega)} = \frac{\omega \sqrt{\epsilon(\omega)}}{c} = \frac{\omega n(\omega)}{c} \vec{e}_k \quad (2.13)$$

Finally we must not forget that the wave number could be a complex number, therefore we could have

$$\vec{k}(\omega) = \beta(\omega) + j \frac{\alpha(\omega)}{2} \quad (2.14)$$

where  $\beta(\omega)$  would be the propagation coefficient of the wave a function of  $\omega$ , and  $\alpha(\omega)$  would be the absorption coefficient of the wave.

## 2.2 Properties of Ultrashort Laser Pulses

Once we have seen some of the most important properties of a electromagnetic wave is easy to define what is an ultrashort laser pulse, since it has an electric field as we have seen above  $\vec{E}(\vec{r}, t)$ .

An ultrashort laser pulse is just a portion of a sine wave, created by multiplying a sine wave and a pulse-envelope function. So, an ultrashort pulse is not much different respect to the other lasers. Furthermore, having a shorter pulses in time, we will have more bandwidth in frequency (spectrum). But a broader spectrum means a greater range of colors, the bandwidth, that we have. And although we are going to deal with pulses whose duration is too short, that color can change fastly during one of them. This color change is the frequency variation, contained in the pulse phase.

And measuring the phase from an ultrashort laser pulse is not easy at all. Indeed, some techniques developed during many years for measuring ultrashort laser pulses before FROG were invented, failed when they treated to get the pulse's phase, unsuccessfully. It is so hard to measure the phase because when the pulse pass through a material its phase can be changed. Several types of glasses are used

to variate the pulse's phase (as fused silica or BK7), and it can also be changed by the air [5].

Then we want to measure the frequency variation (phase) and also the intensity variations of our ultrashort pulse, in order to completely characterize the pulse we are measuring.

## 2.2.1 The Intensity and Phase vs. Time and Frequency

### Intensity and Phase vs. Time

We are going to simplify the electric field expression using the *scalar approximation*, in which we will only care about the temporal features. So the equation above changes to

$$E(t) = \frac{1}{2} \sqrt{I(t)} e^{j(\omega t - \phi(t))} + c.c. \quad (2.15)$$

where  $I(t)$  is the intensity a function of time,  $\phi(t)$  is the phase of the pulse, and  $\omega_0$  is a carrier angular frequency on the order of femtoseconds. Since  $I(t)$  and  $\phi(t)$  vary slowly respect to  $e^{j\omega_0 t}$  we can approximate to a complex pulse field eliminating the c.c. term.

Given the approximation before we can conclude that the temporal intensity and phase are:

$$I(t) = |E(t)|^2 \quad (2.16)$$

We do not care about the absolute magnitude of the intensity, we only are interested about the shape, so, in the equation above we have omitted constants like permittivity  $\epsilon$  and the speed of light  $c$ .

And the phase is:

$$\phi(t) = -\arctan\left(\frac{\Im[E(t)]}{\Re[E(t)]}\right) \quad (2.17)$$

## Intensity and Phase vs. Frequency

Unlike we have done with the temporal Intensity and Phase, where we have taken the complex electric field, for the frequency-domain we have the Fourier Transform of the real electric field. So, from the pulse field in the frequency domain

$$\tilde{E}(\omega) = \sqrt{S(\omega)}e^{-j\phi(\omega)} \quad (2.18)$$

we can obtain the spectral phase and intensity

$$S(\omega) = |\tilde{E}(\omega)|^2 \quad (2.19)$$

$$\phi(\omega) = -\arctan\left(\frac{\Im[\tilde{E}(\omega)]}{\Re[\tilde{E}(\omega)]}\right) \quad (2.20)$$

## 2.2.2 Phase distortions in Time and Frequency

### Zeroth-order Phase: The Absolute Phase

Is the same in both domains, frequency and time. Is the relative phase of the carrier wave with respect to the envelope. We won't take it in account since when the pulse is many cycles long, variations in absolute phase shifts the carrier wave from the peak of the envelope just a little, and therefore the pulse field changes just little.

### First-order Phase: A Shift in Time or Frequency

A linear term in the spectral phase corresponds to a shift in time, and a linear term in temporal phase corresponds to a shift in frequency, being the last one more interesting because we do not care about the arrival time of the pulse (just the shape). Anyway the spectral shift is easily measured with other methods.

## Second-order Phase: Linear Chirp

It is a very important effect over the pulse, the variation of its color during its propagation. Material properties, such as dispersion, alter the (phase) relationship between the spectral components of light, effectively separating the different components of the pulse in time. Chirp elongates the pulse in time.

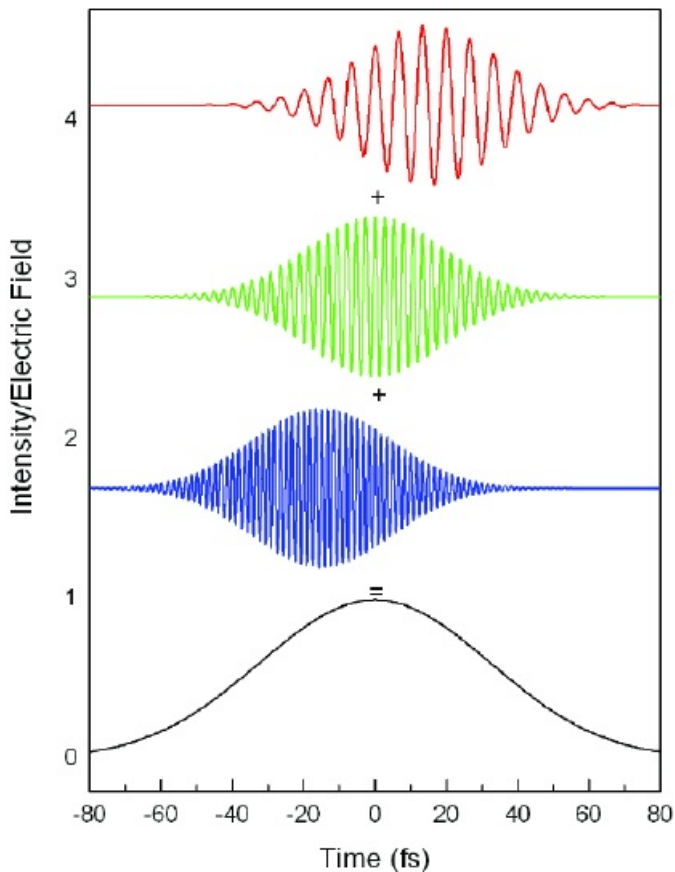


Figure 2.1: Temporal relationship between spectral components of a chirped pulse [18]

Is a quadratic variation of  $\phi(t)$  that represents a linear ramp of frequency vs.time.

$$E(t) = [E_0 e^{-at^2}] e^{jbt^2} \quad (2.21)$$

where  $b$  is the chirp parameter and  $\frac{1}{\sqrt{a}}$  is the pulse duration approximately

$$I(t) = |E_0|^2 e^{-2at^2} \quad (2.22)$$

where  $I(t)$  is the intensity of the linear chirp.

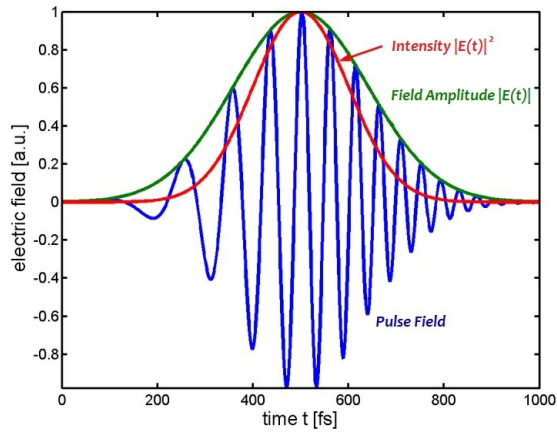


Figure 2.2: Chirped Pulse

A positive linear chirp is usually caused due to the propagation through materials, so a pulse with a negative chirp will be shortened after it has been propagated through material.

### 2.2.3 The Pulse Length and Spectral Width

We want to measure both the intensity and phase of the pulse in time and frequency. We also want to know the pulse shape, and everything we can know regard the pulse, but it is not completely possible. We only can measure approximately the pulse length (width), where the most common definition is the Full-width-half-maximum ( $\tau_{FWHM}$ ).

#### Full-width-half-maximum

Is the time between the most separated points that have half of the peak intensity of the pulse. Is the most intuitive definition and the most used in experiments because is easy to plot it. But is not good for calculations. However, for a simple Gaussian-intensity pulse can be written with ( $\tau_{FWHM}$ )

$$E(t) = E_0 e^{-1.38(\frac{t}{\tau_{FWHM}})^2} \quad (2.23)$$

## 2.3 Nonlinear Optics

It is easy to realize that an ultrashort event in time will provide us a high event in frequency due to the inverse relationship existing between time and frequency domains. It is also interesting to realize that all the energy of an ultrashort laser pulse is contained into a very short time, so they have a very high power and intensity.

Given that we are going to work with high power and intensity pulses, we have to take in account the high-intensity effects that they will suffer. For studying high-intensity effects it is not appropriate to work fall the linear optics area but non-linear optics. Some of these effects are very useful for our work with the FROG as the 'second-harmonic generation' that yields a new frequency twice higher than the input signal.

The fundamental equation of optics is the wave equation:

$$\frac{\partial^2 E}{\partial z^2} - \frac{1}{c_0^2} \frac{\partial^2 E}{\partial t^2} = \mu_0 \frac{\partial^2 P}{\partial t^2} \quad (2.24)$$

where  $\mu_0$  is the magnetic permeability of free space,  $c_0$  is the speed of light in vacuum,  $E$  is the real electric field, and  $P$  is the real induced polarization.  $P$  contains linear-optical effects as the refractive index and the absorption coefficient and also nonlinear-optical effects. At low intensity we have:

$$P = \epsilon_0 \chi^{(1)} E \tag{2.25}$$

where  $\epsilon_0$  is the electric permittivity of free space and  $\chi^{(1)}$  is the linear susceptibility.

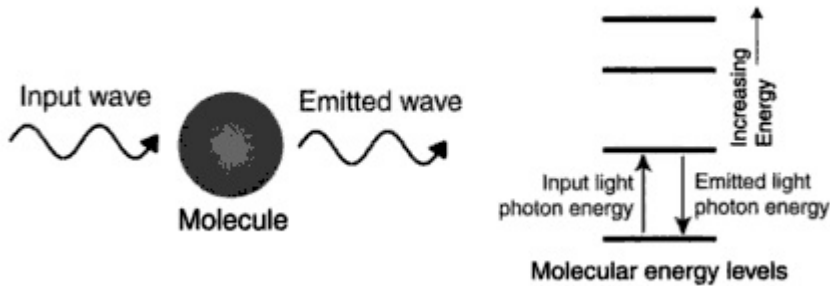


Figure 2.3: Linear optics [6]

In linear optics the wave equation is linear, then  $P$  drives the wave equation to produce light with only those frequencies present in  $P$ , light doesn't change color. As the principle of superposition holds, the beams of light do not affect each other.

## 2.4 Non-linear optical effects

At high intensity, high-order terms must be included to the induced polarization:

$$P = \epsilon_0 \left[ \chi^{(1)} E + \chi^{(2)} E^2 + \chi^{(3)} E^3 + \dots \right] \quad (2.26)$$

If the real field  $E$  is:

$$E(t) = \frac{1}{2} E(t) e^{i\omega t} + \frac{1}{2} E^*(t) e^{-i\omega t} \quad (2.27)$$

and  $E(t)$  is the complex field, squaring this field we have:

$$E^2(t) = \frac{1}{4} E(t) e^{2i\omega t} + \frac{1}{2} E(t) E^*(t) e^{-i\omega t} + \frac{1}{4} E^{*2}(t) e^{-2i\omega t} \quad (2.28)$$

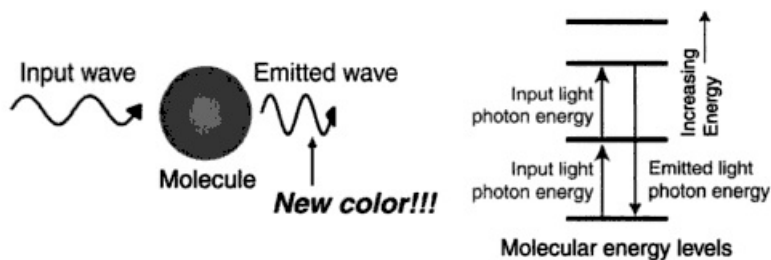


Figure 2.4: Nonlinear optics [6]

This expression includes terms that oscillate at  $2\omega$  the *second harmonic* of the input light frequency, driving the wave equation to yield light at this new frequency. This important process, called *second-harmonic generation* (SHG) permit us create new frequencies and it is the most important effect to measure ultrashort laser pulses.

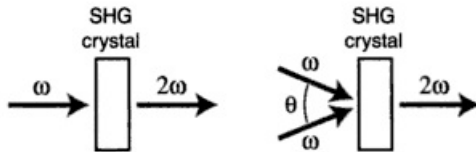


Figure 2.5: Second-harmonic generation

## 2.5 Time-frequency domain

### 2.5.1 Short-Time Fourier Transform

The Fourier transform is a mathematical operation that decomposes a signal into its constituent frequencies. The original signal depends on time, and therefore is called the time domain representation of the signal, whereas the Fourier transform depends on frequency and is called the frequency domain representation of the signal. The term Fourier transform refers both to the frequency domain representation of the signal and the process that transforms the signal to its frequency domain representation.

A window is a mathematical function that is zero-valued outside of some chosen interval. Is used in frequency analysis and signal processing. Some common windows are: rectangular (a), triangular(c), Hanning (e), Hamming (f), cosine, Bartlett, etc.

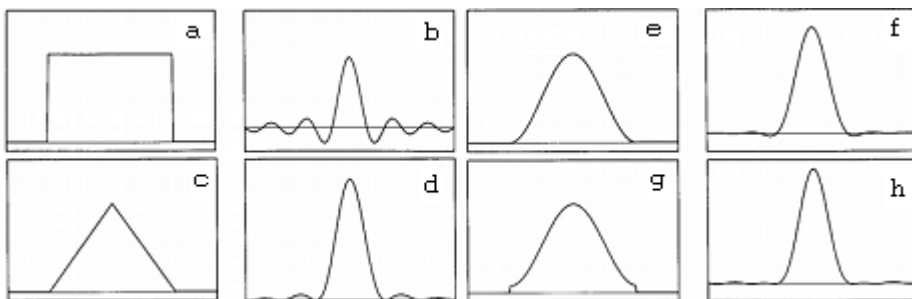


Figure 2.6: Types of windows used for STFT

The windowed Fourier transform replaces the Fourier transform's sinusoidal wave by the product of a sinusoid and a window which is localized in time. It takes two arguments: time and frequency. It is defined by:

$$S_f(t, \omega) = \int_{-\infty}^{+\infty} f(t)g(t - \tau)e^{-j\omega t} dt \quad (2.29)$$

The windowed Fourier transform has a constant time frequency resolution. This resolution can be changed by rescaling the window  $g$ . It is a complete, stable, redundant representation of the signal.

### 2.5.2 Time-Frequency localization

There is no finite energy function which is compactly supported both in the time and frequency domains. The time-frequency localization is measured in the mean squares sense and is represented as a Heisenberg box, which is a rectangle with a time width  $\sigma_t$  and a frequency height  $\sigma_w$ , and time frequency center which coincides with the signal's.

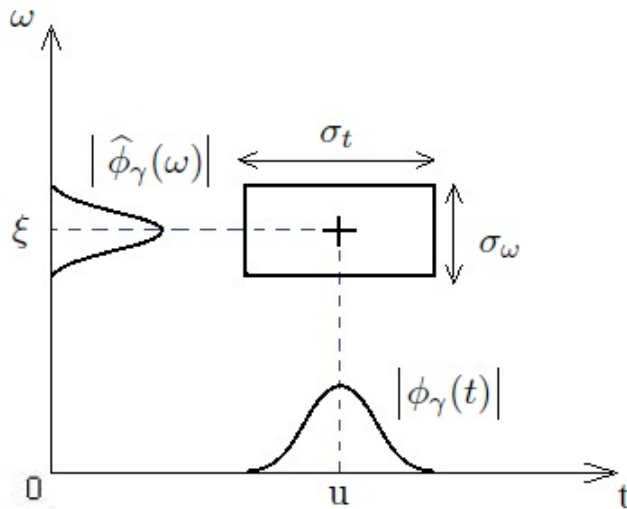


Figure 2.7: Heisenberg box

The Fourier transform can be viewed as a representation of a function as a sum of sinusoidal waves. These sinusoids are localized in the frequency, but not in time, since their support has an infinite length. This is a consequence of periodicity.

To represent the frequency behavior of a signal locally in time, the signal should be analyzed by functions which are localized both in time and frequency, for instance, signals that are compactly supported in the time and Fourier domains. This time-frequency localization is limited by the following two results: *The Uncertainty theorem of Heisenberg* and *Compact Supports*.

### The Uncertainty theorem of Heisenberg

If  $f$  is in  $L^2$ , then its time root deviation  $\sigma_t$  and its Fourier root deviation  $\sigma_w$  are defined. Then

$$\sigma_t^2 \sigma_w^2 \geq \frac{1}{4} \quad (2.30)$$

A balance has to be reached between the time and frequency resolution. In the limit case of a sinusoid,  $\sigma_w$  is zero and  $\sigma_t$  is infinite.

### Compact Supports

If  $f$  is non zero with a compact support, then its Fourier transform cannot be zero on a whole interval. Similarly, if its Fourier transform is compactly supported, then it cannot be zero on a time interval. Hence, even if the Heisenberg constraints are verified, it is impossible to have an function in  $L^2$  which is compactly supported both in the time and Fourier domains. In particular, this means that there is no instantaneous frequency analysis for finite energy signals.

### 2.5.3 The Spectrogram

The square modulus of the windowed Fourier transform is the spectrogram of a signal.

$$|S_f(t, \omega)|^2 = \left| \int_{-\infty}^{+\infty} f(t)g(t - \tau)e^{-j\omega t} dt \right|^2 \quad (2.31)$$

The spectrogram then, shows a visual representation of a signal frequency variations (vertical axis) throughout the time (horizontal axis). This is interesting to know which spectral components of a signal are in each instant of time.

Depending of the window size applied for the Windowed Fourier Transform we will have different resolution levels of the spectrogram. If a very large window size is applied, we will have a great resolution level of spectrogram, however we will also have increased the operation time:

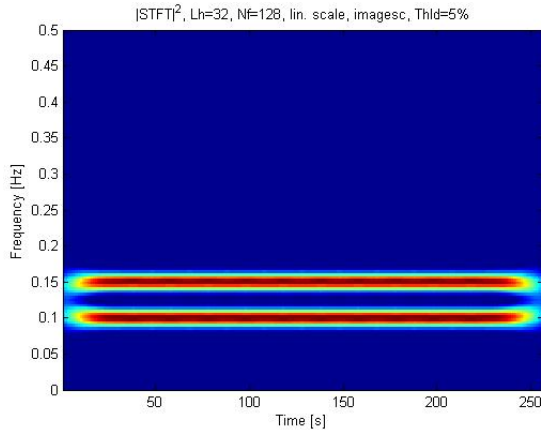


Figure 2.8: Spectrogram with great resolution

On the other hand, if a very short window size is applied, we cannot differentiate the spectral components(at least it will be too hard), but the operation time will decrease.

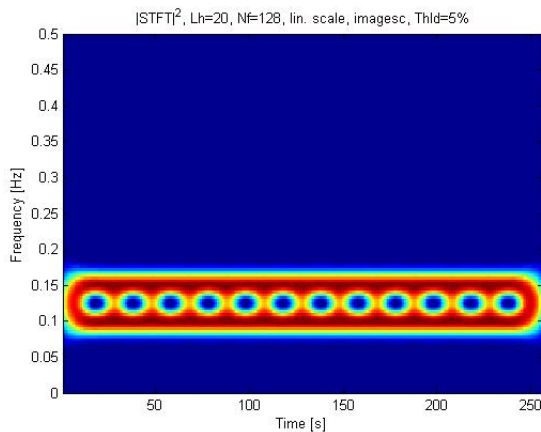


Figure 2.9: Spectrogram with bad resolution

The spectrogram is very useful for identifying two signals that appears added and is too hard to identify each one in the time domain. The next figures show two couples of added signals in time and theirs respective spectrograms.

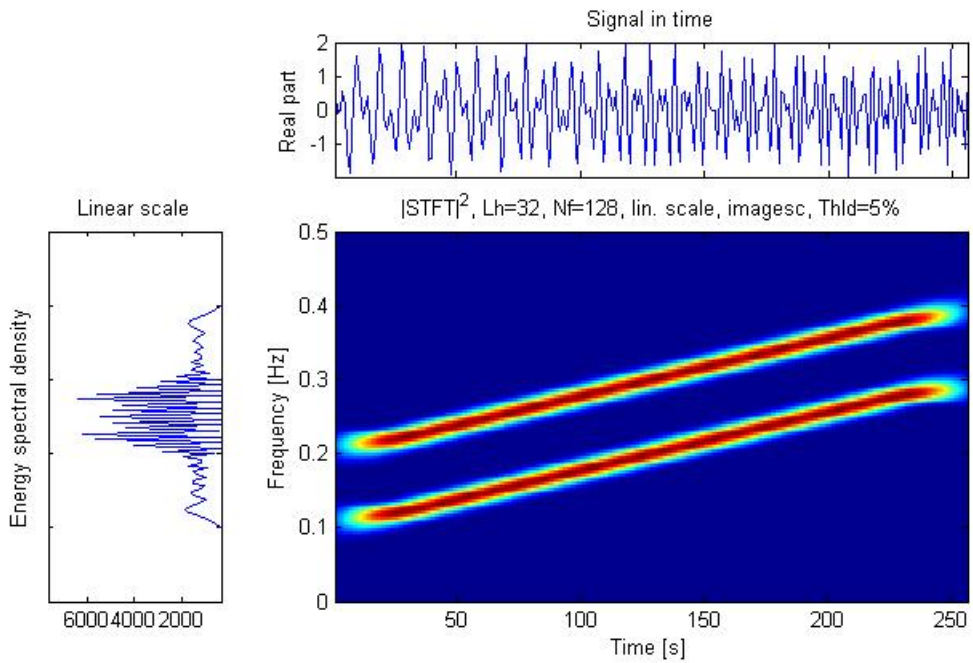


Figure 2.10: Couple of added signals in time 1

We can also see that in frequency-domain is too hard to differentiate the two beams separately in both the graph above and the graph below:

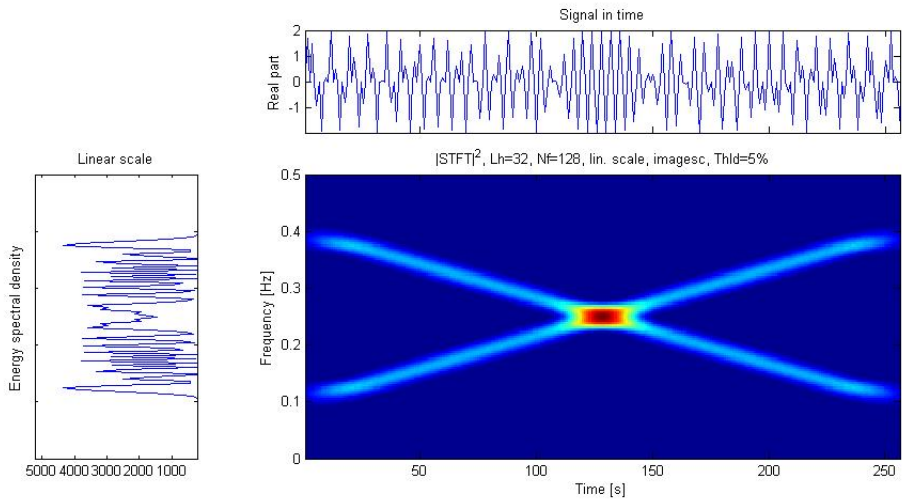


Figure 2.11: Couple of added signals in time 2

As the Windowed Fourier Transform is a FT, and a FT is a sum of several frequency components of a signal, we can see the spectrogram usefulness for this kind of representations and functions. The spectrogram provides us which frequency components are at each instant of time, and this facilitates the study of these signals.

## 2.5.4 Wigner Transform

### STFT limitations

The Windowed Fourier Transform (WFT) or Short-Time Fourier Transform (STFT) (equation 2.32), provides us a good Time-Frequency representation of signals, as we have seen before. But STFT has some limitations due to the nature of the joint time-frequency representation used, given that exist a inverse relationship between time domain and frequency domain, and therefore, between their respective signal resolution.

This is due to a frequency (fourier) domain property, whereby a temporal window and its spectrum cannot both be arbitrarily narrow, because if the window (time) narrows its spectrum widens and then, the signal spectrum resolution gets worse[7].

$$S_f(t, \omega) = \int_{-\infty}^{+\infty} f(t)g(t - \tau)e^{-j\omega t} dt \quad (2.32)$$

The immediate consequence of this inverse relationship between time and frequency is that, using STFT, there is just one way for improving the identification of spectral detail from a spectrogram, and this is achieved impairing the temporal resolution. Therefore, this is not good enough for pulse transmission, so we need another kind of representation for the joint time-frequency that provides us better results for this joint. Is it usually used quadratics representations because this kind of representations have a quadratic (non-linear) relations with the signal, similar to signal-energy relation, thus showing an important signal feature, the energy distribution. Actually we will can see that these quadratic representations have to satisfy some conditions to seem a energy distribution representation. The most basic time-frequency quadratic (bilinear) representation, and object of our study is the Wigner Distribution (WD) (equation 2.33).

### Wigner-Ville Distribution WVD

The Wigner Distribution (WD) was proposed by Eugene Wigner in 1932 for application in quantum mechanics. This distribution was redefined by Ville (WVD-Wigner-Ville Distribution) in 1948 at signal context, like a time-frequency function [8]. It has more recently been recognised as a powerful tool for time-frequency analysis of signals, where with some care, it can be interpreted as a distribution of the signal energy in time and frequency. Claasen and Mecklenbrauker [9] show that the WVD can be evaluated from time signal f(t)

$$W_f(t, \omega) = \int_{-\infty}^{+\infty} f\left(t + \frac{\tau}{2}\right) f^*\left(t - \frac{\tau}{2}\right) e^{-j\omega\tau} d\tau \quad (2.33)$$

While STFT is a linear transform, WVD is a bilinear (non-linear) distribution. The first difference we can appreciate between linear and non-linear representations is the fulfillment or not of Superposition Theorem [10]

$$T[\alpha_1 f_1 + \alpha_2 f_2] = \alpha_1 T[f_1] + \alpha_2 T[f_2] \quad (2.34)$$

Linear representations fulfill Suerposotion Theorem, while non-linear representations do not do it, so WVD neither does it.

### WVD properties

Bilinear representations have to satisfy several conditions to be a valid energy distribution interpretation. WVD is the most complete distribution, satisfying more properties or conditions than any of other distributions.

### Marginal Properties

The spectral density of energy and instant energy (power) can be obtained as WVD marginal distributions

$$\int_{-\infty}^{+\infty} W_f(t, \omega) dt = |F(\omega)|^2 \quad (2.35)$$

$$\int_{-\infty}^{+\infty} W_f(t, \omega) d\omega = |f(t)|^2 \quad (2.36)$$

, being  $|F(\omega)|^2$  the spectral density of energy and  $|f(t)|^2$  the instant energy (power).

### Energy Conservation

To be considered our distribution like a energy density it must satisfy

$$\int_{-\infty}^{+\infty} \int_{-\infty}^{+\infty} W_f(t, \omega) dt d\omega = \int_{-\infty}^{+\infty} |f(t)|^2 dt = \int_{-\infty}^{+\infty} |F(\omega)|^2 d\omega \quad (2.37)$$

### Negativity or Real Property

WVD spectrum always takes real values of the signal. This means that it takes both negative and positive values, so we can conclude WVD cannot be defined as density function, given that WVD spectrum should have only positive values to be a density function[6].

### Invariance Properties

We have

$$s(t) = f(t - t_0) \tag{2.38}$$

$$s(t) = f(t)e^{-j\omega_0 t} \tag{2.39}$$

If  $s(t)$  is equal to  $f(t)$  time-shifted or frequency-shifted function the signal is invariant to time or frequency shifts, respectively, when

$$W_s(t, \omega) = W_f(t - t_0, \omega) \tag{2.40}$$

$$W_s(t, \omega) = W_f(t, \omega - \omega_0) \tag{2.41}$$

## 2.6 WVD Drawbacks and conclusions

The main drawback of WVD and any bilinear time-frequency distribution representation is the interference between the own terms of the distribution and its crossed terms. This crossed terms are generated due to the quadratic nature of WVD, that it has several spectral components. The crossed terms are always generated for any kind of signal or noise (each signal has their own crossed term), and it may induce to misleading representation and impair the useful signal analysis[11].

It can be shown that the WVD is the most basic distribution. Another important attribute is the spread of the square magnitude of any joint time-frequency distribution. It can also be shown that in the case of the WVD, the spread will be smaller and easier reduced than of the STFT[12-13].

## Chapter 3

# Previous alternatives techniques of measuring

It has been said in previous lines that, in order to measure a pulse, we need to get its intensity and phase in either the time or frequency domains. And, before the FROG appearance, it was done with autocorrelation (time-domain) and spectrum (frequency-domain).

We are going to see the FROG technique is a more complete solution for measuring ultrashort pulses than autocorrelation and spectrum separately. But we hardly need to know the features of those previous alternatives of measuring ultrashort pulses, since as we are going to see in next chapters, the Frequency-Resolved Optical Gating is strongly based on them.

### 3.1 The Spectrum

The target in the frequency domain is the spectrum, as we mentioned above. There are some devices that can get the spectrum, they are the spectrometer and the interferometer. There are several ways to perform a spectrometer either diffraction-grating device or Fourier-transform spectrometers.

The last ones operate in the time domain and measure the transmitted integrated intensity from a Michelson interferometer, often called the light's second-order coherence function, also called the interferogram and the field autocorrelation:

$$\Gamma^{(2)}(\tau) = \int_{-\infty}^{+\infty} E(t)E^*(t - \tau)dt \quad (3.1)$$

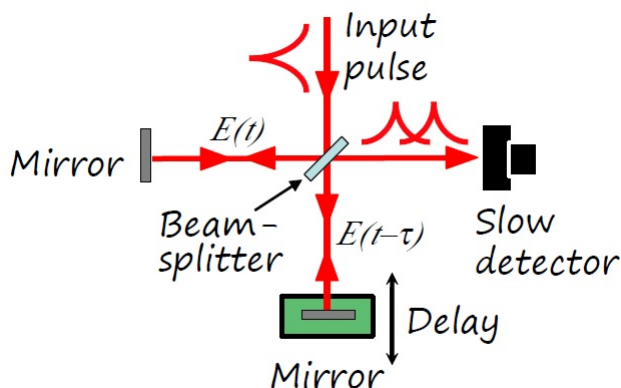


Figure 3.1: Michelson's interferometer [6]

And its Fourier transform gives the spectrum, the Autocorrelation Theorem:

$$|\tilde{E}(\omega)|^2 = F \left\{ \int_{-\infty}^{+\infty} E(t)E^*(t - \tau)dt \right\} \quad (3.2)$$

### One-Dimensional Phase Retrieval

We have seen that we can get the spectrum, but just this, the spectrum. We cannot get the spectral phase easily, since there are too many pulses that correspond to a given spectrum. However, if we have available some additional information as the kind of event we are measuring (a pulse) and the knowledge that the pulse intensity in time domain is zero outside a finite range of times, we could reduce the number of possible pulses candidates to correspond to our given spectrum.

We are dealing then with a one-dimensional phase-retrieval problem, since we want to retrieve the spectral phase from the spectrum using additional information.

Nevertheless, even with the additional information, the one-dimensional phase-retrieval problem is usually unsolvable. With the constraints that we could fix, we reduce the number of possible corresponding pulses, but it is not enough, there would still be infinite possibilities.

Some of the reasons for this large amount of pulses that can correspond to the same spectrum magnitude are the 'trivial' ambiguities [14]. For example, adding a phase shift to a spectrum belonging to a complex amplitude we still have the same spectrum:

$$E(t) \implies \text{Absolute-phase shift} \implies E(t)e^{i\phi_0}$$

It occurs the same with two more ambiguities:

$$E(t) \implies \text{Time translation} \implies E(t - t_0)$$

$$E(t) \implies \text{Time-reversal} \implies E^*(-t)$$

But those are just the *trivial* ambiguities, there are more complex ambiguities we cannot live with. The number of ambiguities associated with the measurement of the pulse spectrum are too many.

We could have a *sech*<sup>2</sup> spectrum with a chirp parameter, and it can correspond to another *sech*<sup>2</sup> in time domain, but with any pulse width.

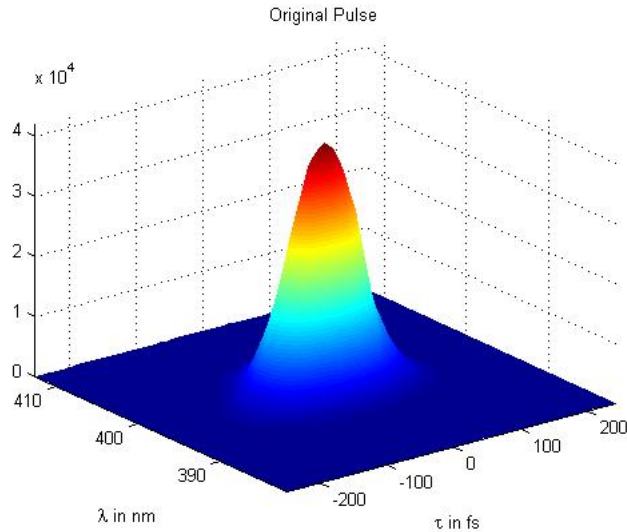


Figure 3.2: Example of  $\text{sech}^2$  pulse

## 3.2 The Intensity Autocorrelation

The intensity autocorrelation results when a pulse is used to measure itself in the time domain [15]. In order to measure the pulses's intensity in time domain we need a shorter event than the pulse we want to measure. If we have not got that shorter event, we have to use the pulse to measure itself as we have said above.

It is so interesting to know how the intensity autocorrelation is done because it is gonna be quite similar to the FROG setup that we are gonna see in following chapters. Firstly, the pulse is splitting into two arms, after that one of them is delayed respect the other one. Finally we have to overlap both arms spatially in a nonlinear-optical medium such a second-harmonic generation crystal(SHG). In order to get the second-harmonic in my FROG setup, I use a beta Barium Borate (BBO) crystal.

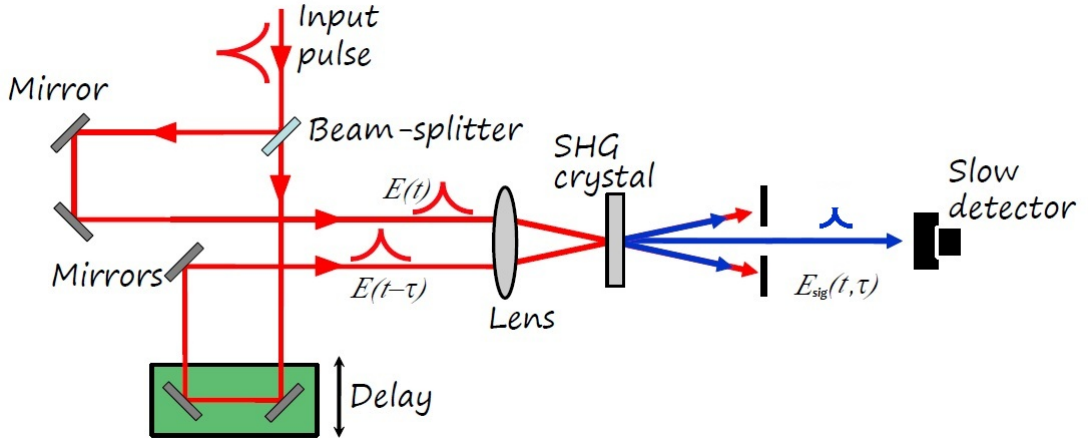


Figure 3.3: Intensity Autocorrelator [6]

The light that is produced by the SHG crystal is twice the frequency input light. In my experiments I use a fundamental light of  $\lambda = 800 \text{ nm}$  (red light), and the BBO produces a  $400 \text{ nm}$  light (blue). The field and its intensity are given as:

$$E_{sig}^{SHG}(t, \tau) \propto E(t)E(t - \tau) \quad (3.3)$$

$$I_{sig}^{SHG}(t, \tau) \propto I(t)I(t - \tau) \quad (3.4)$$

The detector used at the end of the autocorrelator setup is too slow to resolve in time the intensity autocorrelation, so this measurement produces a time integral[10]:

$$A^{(2)}(\tau) = \int_{-\infty}^{+\infty} I(t)I(t - \tau)dt \quad (3.5)$$

That is the intensity autocorrelation, similar to the field autocorrelation equation we talk about before (equation 3.1), but not the same at all, since its information is related with the spectrum. It is needed an autocorrelation to overlap pulses in time and then, we can get a measure of a second-harmonic pulse's length. If there is a relative delay of one pulse length, the second-harmonic generated intensity will be decreased.

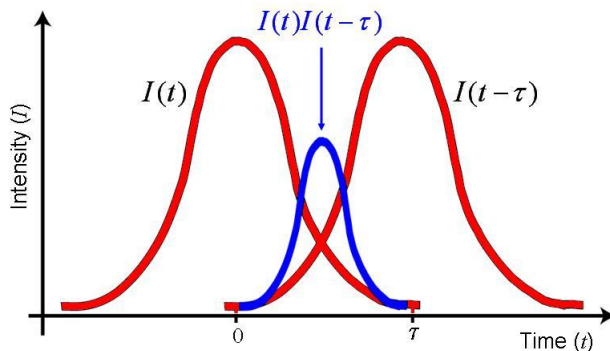


Figure 3.4: Autocorrelation [6]

The autocorrelation is symmetrical, if we replace  $\tau$  by  $-\tau$  in equation 3.4 we obtain  $A^{(2)}(\tau) = A^{(2)}(-\tau)$ . So it cannot be distinguished a pulse from its mirror image:

$$A^{(2)}(\tau) = \int_{-\infty}^{+\infty} I(t + \tau)I(t)dt \quad (3.6)$$

The Fourier transform of the autocorrelation is the mag-squared Fourier transform of the intensity:

$$\tilde{A}^{(2)}(\omega) = |\tilde{I}(\omega)|^2 \quad (3.7)$$

We could see there are some constraints that we can apply in order to reduce the number of possibilities to find  $I(t)$  from the Fourier transform of the autocorrelation, as the fact  $\tilde{A}^{(2)}(\omega)$  is real and non-negative. Nevertheless, the autocorrelation gives us the magnitude, but not the phase of Fourier transform of  $I(t)$ . There is again a one-dimensional phase-retrieval problem, with trivial ambiguities and stronger

constraints than before, I mean respect to the spectrum's one-dimensional phase-retrieval problem. The target in this case is supposed to be easier to reach respect to the spectrum's goal, as well known, it was obtaining the complete pulse field. Now, we only want to get the pulse intensity  $I(t)$ .

### Pulse Length

Well, the autocorrelation cannot give us the intensity without dealing with a lot of ambiguities and their corresponding assumptions, but it could provide us useful information, as the pulse length.

The rms (root mean square) pulse length is easy to get from the autocorrelation by using a known result in probability theory that, if we have a convolution,  $h(t) = f(t) * g(t)$  the rms widths of the functions belonging to the convolution are related by a Pythagorean sum[16]:

$$(\tau_{rms})_h^2 = (\tau_{rms})_f^2 + (\tau_{rms})_g^2 \quad (3.8)$$

The autocorrelation is a kind of autoconvolution, with an argument reversed  $A^{(2)}(t) = I(t) * I(-t)$ :

$$(\tau_{rms})_A^2 = 2(\tau_{rms})^2 \quad (3.9)$$

That is good, but we normally prefer to work with FWHM (Full-Width Half-Maximum) instead since rms is too sensitive in the pulse wings, and we do not like it. But in this case, the autocorrelation does not provide much information, so we have to make a guess about the pulse shape and then deriving a multiplicative factor that relates the autocorrelation FWHM with the autocorrelation of the pulse  $I(t)$ . This factor varies depending the pulse shape taken, being for a Gaussian intensity 1.41, and for a  $sech^2(t)$  1.54 times wider.

### 3.3 Combination of Autocorrelation and Spectrum

We have seen that neither the autocorrelation or spectrum provide a complete pulse field. But we could use both to try it, taking in account that they can strongly constraints each other about their respective one-dimensional phase-retrieval problems.

Rundquist and Peatross did it [17]. They realized that knowing intensity and spectrum, is often enough to provide the phase in both domains. But for ultra-short laser pulses we have the autocorrelation, instead of the intensity, and the spectrum. So the same problem than before remains.

Summarizing, maybe the autocorrelation and spectrum could not measure ultra-short pulses very well, but they have been the best results until better techniques were discovered or invented.

## Chapter 4

# Frequency-Resolved Optical-Gating (FROG)

### 4.1 Introduction and principal features

Finally, here it is. The *Frequency-Resolved Optical-Gating* appears to solve the problems that autocorrelation and spectrum could not, neither separately or both together.

FROG measures a spectrogram of the pulse. We have seen in chapter 2 a couple of Time-Frequency domain distributions, one of them is the spectrogram. Recalling that chapter, we should know that a knowledge of the spectrogram of  $E(t)$  is enough to completely determine  $E(t)$ , except some *trivial* ambiguities.

We have to remind that spectrogram uses a gate function for gating the field  $E(t)$ . As occurs in autocorrelation, we have to use the pulse to measure itself, in this case, to gate itself. After that we will have to solve in frequency domain the gated piece of the pulse.

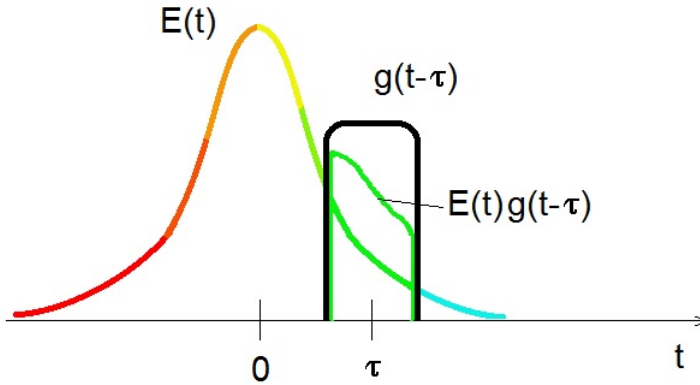


Figure 4.1: Description of the spectrogram

We must compute the spectrum of the product  $E(t)g(t - \tau)$ , where  $E(t)$  contributes phase (i.e., color) to the signal pulse and  $g(t - \tau)$  contributes only intensity, not phase. The spectrogram yields the color and intensity of  $E(t)$  at the time  $\tau$ .

Yes, it seems similar to autocorrelation, but now we also have a spectral resolution and that will make the difference. That is true, we have to gate a unknown pulse with itself, a gate also unknown so we could not use available spectrogram inversion algorithms. So, finally, we can say that FROG is basically an autocorrelation measurement, whose output is spectrally solved, the difference is that from now, we are not going to measure the autocorelation energy along the time domain, but the spectrum along the time.

An example of a FROG trace could be:

$$I_{FROG}^{SHG}(\omega, \tau) = \left| \int_{-\infty}^{\infty} E(t)E(t - \tau)e^{-j\omega t} dt \right|^2. \quad (4.1)$$

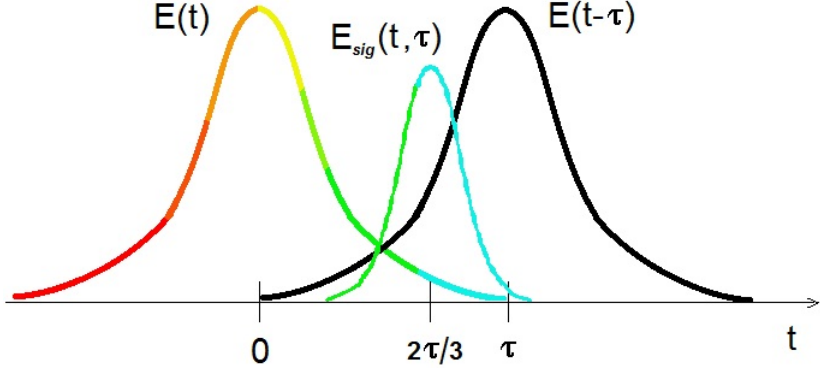


Figure 4.2: FROG signal

It is interesting to see that the FROG trace is a spectrogram in which the pulse intensity gates itself where the gate function here is  $E(t - \tau)$ . In order to obtain  $E(t)$  from its FROG trace we have to consider that  $E_{sig}(t, \tau) \propto E(t)E(t - \tau)$  is considered as the Fourier transform with respect to  $\tau$ , of a new quantity called  $\bar{E}_{sig}(t, \Omega)$ :

$$E_{sig}(t, \tau) = \int_{-\infty}^{\infty} \bar{E}_{sig}(t, \Omega) e^{-j\Omega\tau} d\Omega \quad (4.2)$$

So, once we have found either  $E_{sig}(t, \tau)$  or  $\bar{E}_{sig}(t, \Omega)$  the pulse field  $E(t)$  is given. So, to find  $E(t)$  we just need to know  $\bar{E}_{sig}(t, \Omega)$ , then if we substitute the equation into the FROG trace we have:

$$I_{FROG}^{SHG}(\omega, \tau) = \left| \int_{-\infty}^{\infty} \int_{-\infty}^{\infty} \bar{E}_{sig}(t, \Omega) e^{-j\omega t - j\Omega\tau} dt d\Omega \right|^2. \quad (4.3)$$

This expression yields the magnitude, but not the phase. So the problem now is to find the phase of  $\bar{E}_{sig}(t, \Omega)$ , being known this inversion problem as the two-dimensional phase-retrieval problem.

The difference between the two-dimensional phase-retrieval problem and the one-dimensional phase-retrieval problem is that, the first one has, however, a unique solution and is a solved problem when certain additional information about  $\overline{E}_{sig}(t, \Omega)$  is available, while in the one-dimensional phase-retrieval problem many solutions can exist. Furthermore, the two-dimensional phase retrieval problem has only *trivial* ambiguities:

$$\overline{E}_{sig}(t, \Omega) \implies \text{Absolute phase factor} \implies \overline{E}_{sig} e^{i\phi_0}$$

$$\overline{E}_{sig}(t, \Omega) \implies \text{Time translation} \implies \overline{E}_{sig}(t - t_0, \Omega - \Omega_0)$$

$$\overline{E}_{sig}(t, \Omega) \implies \text{Time-reversal} \implies \overline{E}_{sig}^*(-t)$$

Is too hard that another solution may exist, but it normally does not occur. It is important to say that using an iterative algorithm, the pulse field  $E(t)$  could be determined. I won't go into any algorithm performance, for a deeper study of the FROG algorithm is highly recommended Trebino's book, chapter 8[15]. But it is interesting to know how works a generic algorithm, given that we are gonna use that later to retrieve the pulse field  $E(t)$  from its FROG trace:

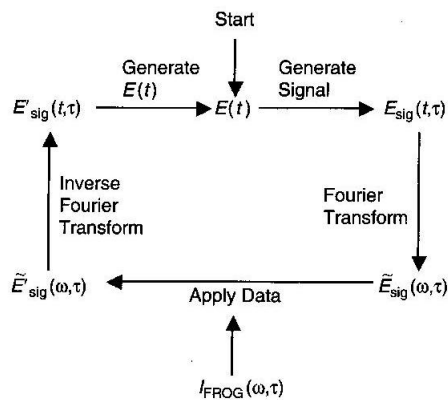


Figure 4.3: Schematic of a generic FROG algorithm[15]

## 4.2 Properties and advantages of FROG

We have seen that the most important property of FROG is that we can get the pulse intensity and phase either estimating by looking at experimental FROG trace or using the iterative algorithm to retrieve the precise values of intensity and phase versus time or frequency.

FROG is highly accurate, especially for measuring the phase in the wings of the pulse. It is experimentally simple and very general, we can use FROG to measure simple and complex pulses. FROG can measure a wide range of pulse lengths, from a few femtoseconds to many picoseconds.

It operates from the mid-infrared region to the Ultra-Violet. FROG operates single-shot or multi-shot, and it's very sensitive, Spectrograms for Linearly Chirped Pulses 1-pJ pulses in multi-shot and  $1 - \mu J$  in single-shot. FROG is insensitive to noise, for a 10% of additive noise it is produced an error in intensity and phase less than 1%. FROG overdetermines the pulse, revealing potentials systematic errors and it can correct them, even when their causes are unknown. FROG is rigorous and well established, is really fast and it can measure two pulses at the same time.

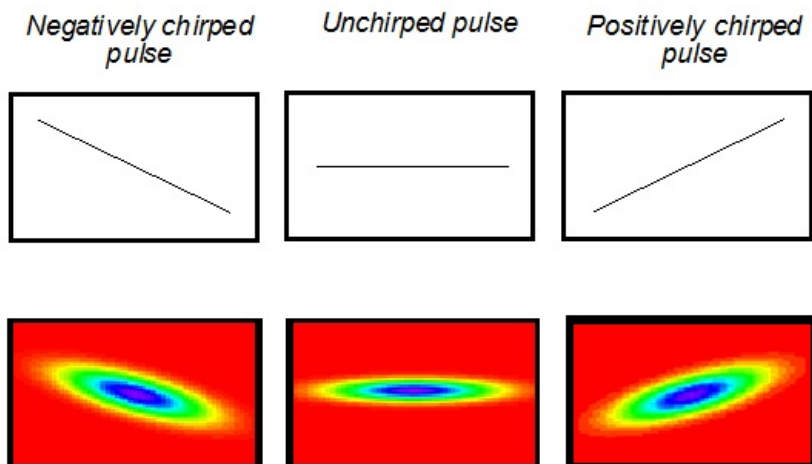


Figure 4.4: Spectrograms for Linearly Chirped Pulses [6]

## 4.3 Impairments

We can agree in the fact tha FROG is a powerful tool to measure ultrashort laser pulses, but there some aspects of intensity and phase that it cannot measure. FROG doesn't measure the absolute phase,  $\phi_0$  in the Taylor expansion of spectral phase, since it is a mag-squared magnitude. As the pulse is gating itself, there is no absolute time reference, so it cannot measure, for example, the arrival time,  $\phi_1$ , the firs-order term coefficient in the spectral-phase Taylor series.

# Chapter 5

## FROG Device Setup

### 5.1 The Ti:Sapphire laser

Before starting with the FROG Device, it is interesting to mention where our fundamental beam comes from. And it comes from a Ti:Sapphire laser.

Since their invention in the early 1980s, titanium-doped sapphire (Ti:Al<sub>2</sub>O<sub>3</sub> or Ti:sapphire) lasers and amplifiers have enabled countless applications in fundamental research in physics, biology and chemistry. Today, they play an important role across a wide range of photonics applications, including multicolor ultrafast spectroscopy, multiphoton deep-tissue imaging, terawatt and petawatt physics [19].

Compared with other competing media, the Ti:sapphire medium is extremely flexible and provides high performance and several advantages. It is unmatched in its characteristics for delivering a combination of broad spectral bandwidth, a range of repetition rates, wide tunability and high-average-power levels. Spectral outputs of Ti:sapphire lasers range from ultranarrow single frequency to several hundred nanometers of bandwidth, resulting in ultrafast pulses as short as a few oscillations of the electric field at 5.5 *fs*. At the same time, repetition rates can range from single-shot output for maximum energy up to multigigahertz quasi-CW output with tunability of 400 *nm* and average powers of many watts.

### 5.2 Second-Harmonic-Generation FROG

#### 5.2.1 FROG Beam Geometries

One of the properties of FROG is its versatility, and because FROG is a spectrally resolved autocorrelation, every nonlinear-optical process available to make several types of autocorrelator can also be used to make different kinds of FROG.

I am not going to talk about the different beam geometries of FROG, we only have to pay attention in this thesis to the SHG nonlinear-effect and its FROG configuration. Anyway in Trebino's book [6] there is a complete chapter dedicated to this topic. Anyway, here I leave a summary-table:

			<b>Sensitivity</b>	<b>Ambiguities</b>	
Second-harmonic generation	<b>SHG</b>		.001 nJ	Direction of time; Rel. phase of multiple pulses	most sensitive; most accurate
Third-harmonic generation	<b>THG</b>		1 nJ	Relative phase of multiple pulses	tightly focused beams
Transient-grating	<b>TG</b>		10 nJ	None	useful for UV & transient-grating experiments
Polarization-gate	<b>PG</b>		100 nJ	None	simple, intuitive, best scheme for amplified pulses
Self-diffraction	<b>SD</b>		1000 nJ	None	useful for UV

Figure 5.1: Different FROG geometries. The prism/lens represents a spectrometer[6]

The third order FROG geometries (Polarization Gating (PG), Self-Diffraction (SD), Transient Grating (TG)) give traces in time-frequency domain whose spectral components can belong to a different instants of time. SHG gives symmetrical traces, so it is less intuitive the correspondence between the spectral components and the instants of time. Third-harmonic generation (THG) is intermediate between the two above cases.

## 5.2.2 SHG FROG

My whole work in the laboratory goes around the SHG FROG, and as we saw in equation 4.1, it is based in a SHG autocorrelator, spectrally resolved.

The main advantage of SHG FROG is sensitivity, unlike the other geometries with SHG FROG we just have to deal with a only second-order nonlinearity. It is commonly used to measure unamplified pulses directly from a Ti:Shapphire oscillator, as I did.

SHG FROG also gives the best signal-to-noise ratios because of its different signal beam colour and it is also ideal for few-femtoseconds pulse measurement.

The main drawback of SHG FROG, as we said before, is that it has unintuitive traces, symmetrical with respect to delay, and that means there is an ambiguity in the direction of time that can be removed easily if wanted.

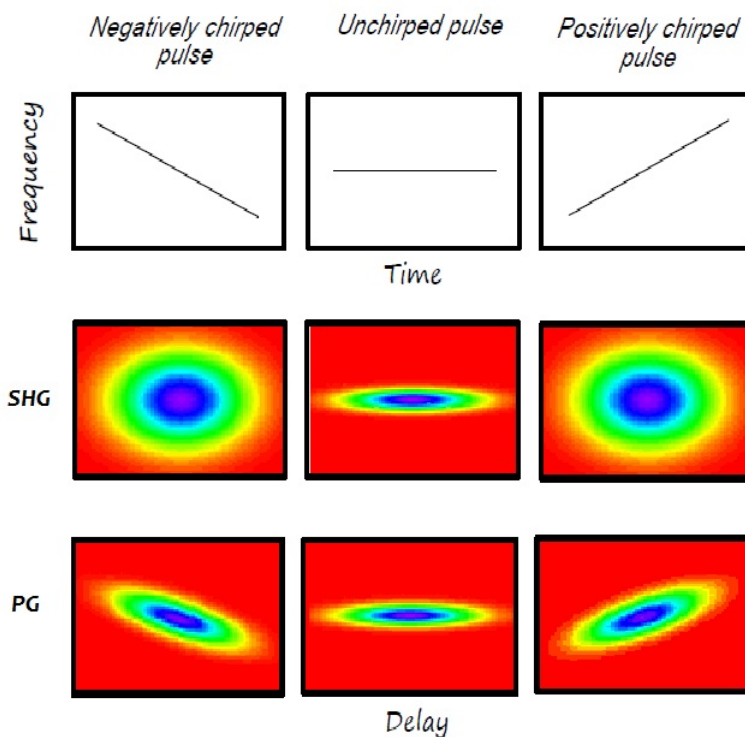


Figure 5.2: Difference between SHG and PG traces [6]

The most important experimental thing that we have to take care about, is the SHG crystal bandwidth, since it is inversely proportional to the crystal thickness. If the crystal is too thick the SHG FROG trace will be too narrow along the spectral axis, resulting to a non-convergence of the algorithm.

The picture below shows an experimental setup for a SHG FROG device, with a 50/50 beamsplitter, a delay line using two mirror pairs on translation stages to give variable delays, a focal lens/mirror to focus the pulses into the SHG crystal (KDP or BBO), and a spectrometer camera. For BBO (Beta Batium Borate) crystal is recommended a  $\approx 100 \mu\text{m}$  thickness, in order to measure 100-femtoseconds pulses.

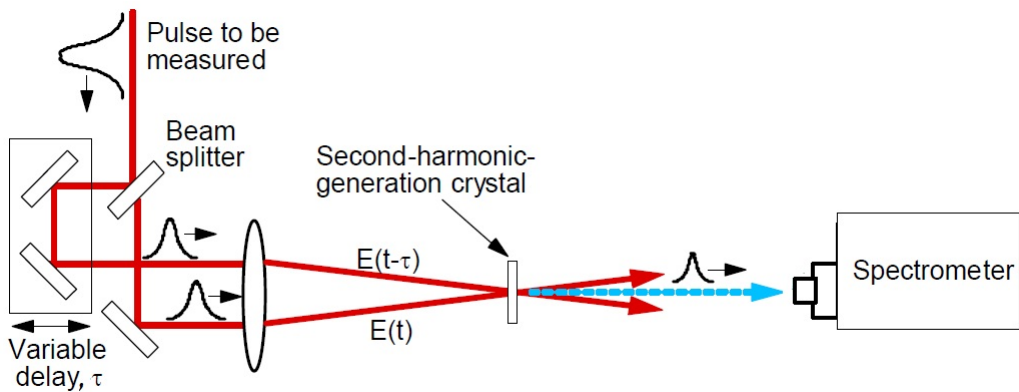


Figure 5.3: SHG FROG experimental setup [6]

### 5.3 Setting-up SHG FROG Device

We saw in the section above a possible experimental SHG FROG device schematic, but it is not the one. Before starting with the description of the setup that I have done, is important to clarify that there are several possibilities for building a SHG FROG device, depending, for example, of the optic material available or space at workplace. For my setup I have followed the Newport (our optics provider company) approach.

Short name	Name	Model
<b>BS1</b>	Beamsplitter	10RQ00UB.2
<b>BS2</b>	Beamsplitter	10RQ00UB.2
<b>WP</b>	$\frac{\lambda}{2}$ Waveplate	10RP52-1
<b>IA1</b>	Iris Assembly 1	ID-0.5
<b>Pell</b>	Pellicle Beamsplitter	PBS-2C
<b>DL1</b>	Delay Line 1	10SD520ER.2
<b>DL2</b>	Delay Line 2	10B20UF.20
<b>FM</b>	Folding Mirror	20D20ER.2
<b>CM</b>	Spherical Mirror	20DC500ER.2
<b>BBO</b>	Nonlinear crystal (Castech)	H6825-1
<b>DF</b>	Dichroic Filter	FSR-KG5
<b>IA2</b>	Iris Assembly 2	ID-1.0
<b>MC</b>	Motion Controller	SMC100CC
<b>MS</b>	Minispectrometer	78358

Table 5.1: Frog device's subassemblies and optics

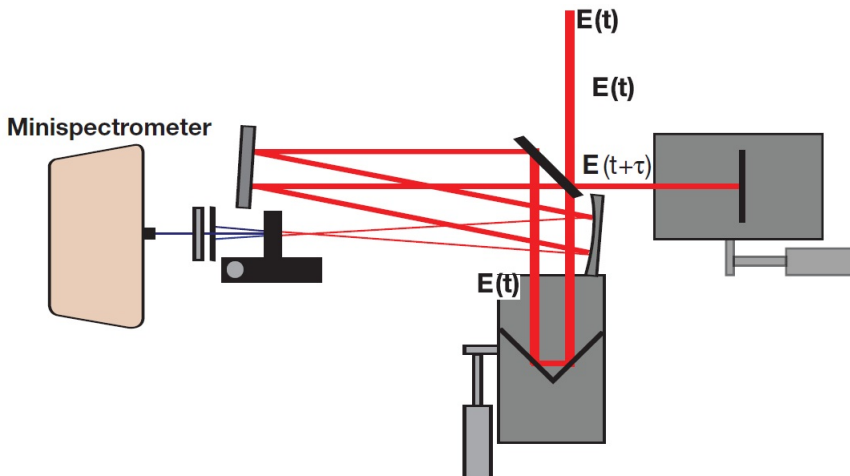


Figure 5.4: SHG FROG Schematic of Newport [18]

Throughout the project I have used a lot of useful tools as posts, holders, aligning stuff, but I am not going to specify all the instruments, just the the most important, they are the optics. The table 5.1 shows the principal optics and assemblies needed to set up the SHG FROG.

The first step to be done is to achieve that the fundamental beam from the

Ti:Sapphire laser, our laser, gets the FROG device. It is important to take in account the sensitivity of our spectrometer, since the Ti:Sapphire provides a 400 mW beam, and it could damage the spectrometer if we are not careful. If the beam is low enough than the spectrometer sensitivity, we would only need some mirrors in order to drive the beam towards the FROG setup.

So, we have to calculate the sensitivity of our spectrometer, and it is easy to get from its power features availables in the spectrometer's data sheet:

Power average of the output beam from the Ti:Sapphire laser  $\Rightarrow P_{av} = 400 \text{ mW}$

For calculating the sensitivity of our autocorrelator we did:

Repetition rate =  $80.38 \text{ MHz} \Rightarrow T_{rep} = \frac{1}{8.38 \cdot 10^6 \approx 12 \mu s}$

$$P_{av} T_{rep} = P_p t_p$$

$$P_p = \frac{P_{av} T_{rep}}{t_p}$$

$$P_p = \frac{400 \cdot 10^{-3}}{60 \cdot 10^{-15} \cdot 8.38 \cdot 10^6} \text{ Watts}$$

$$P_p \approx 10^5 \text{ W}$$

$$P_{av} P_p = 400 \cdot 10^{-3} \cdot 10^5 \cong 4 \cdot 10^4 \text{ W}^2$$

$$\text{Autocorrelator Sensitivity} = 4 \cdot 10^{-4} \text{ W}^2$$

But in this case, we have to calculate the sensitivity of our spectrometer, and it is easier to get, since we can get the value that we need from its power features availables in the spectrometer's data sheet:

Power Density, Average Maximum with Atenuator  $\Rightarrow P_{DEN} = 0.2 \frac{\text{W}}{\text{cm}^2}$

$$P_{av} = P_{DEN} \cdot \text{Detector Active Area} = 0.2 \frac{\text{W}}{\text{cm}^2} \cdot 1 \text{ cm}^2$$

$$P_{av} = 200 \text{ mW}$$

So our spectrometer has a sensitivity of 200 mW, so we will have to use some beamsplitters along the path of the fundamental beam. I had available at the laboratory differents beamsplitters with their respectives transmitted/reflected ratios. I just chose two of them, a 85%/15% beamsplitter (BS1) and a 35%/65% beam-splitter (BS2). That would give me a low enough input power at the entrance of the FROG device.

With this configuration, the beam does not go through any beamsplitter before going into the FROG device, we are just using the reflected beam in both beamsplitters. What if we had needed to put the FROG device behind the transmitted part of a beamsplitter? In order to ensure that during the beam routing the beamsplitters do not add an important amount of dispersion to the beam it should be interesting check it, and I did it.

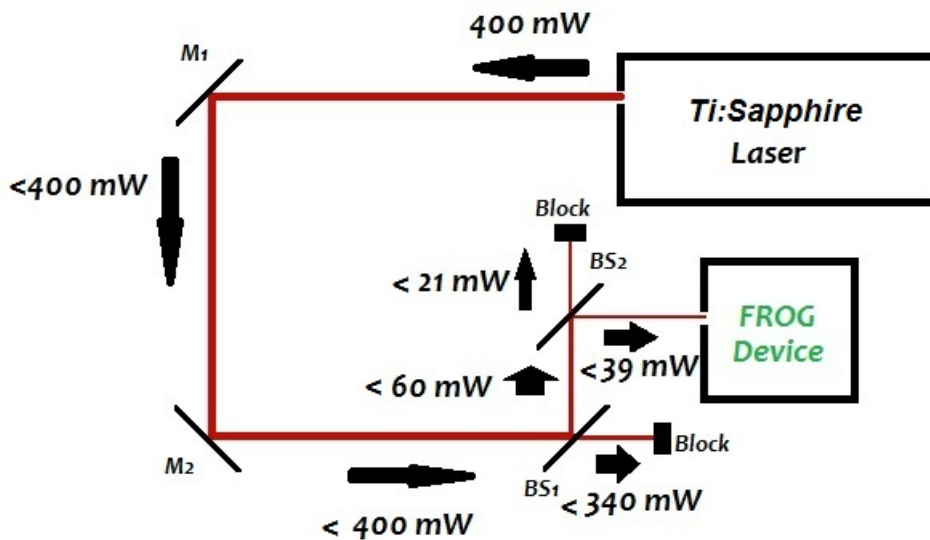


Figure 5.5: Previous Routing Beam

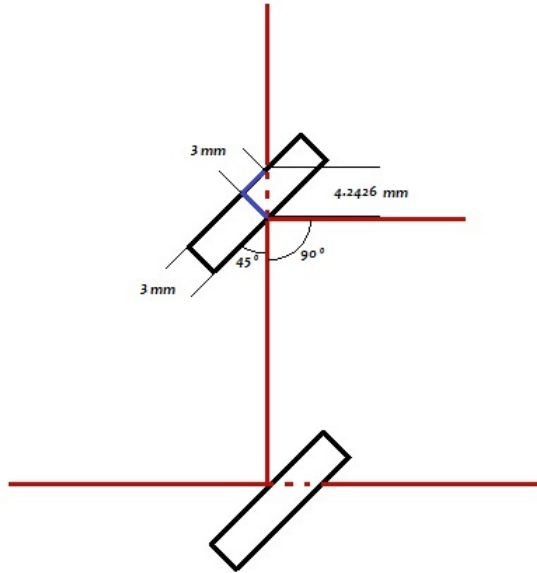


Figure 5.6: Quantity of light that goes through the beamsplitter

Well, the beam only goes through one of the two beamsplitters with an angle of incidence of 45, what mean that we have a right angle, and the Pythagorean theorem with two legs (two sides of the right angle) of 3 mm, we need to get the hypotenuse:

$$x^2 = 3^2 + 3^2(mm) \quad x = \sqrt{9 + 9}(mm) \quad x = 4.2624(mm)$$

And now if we use the next equation to know the new FWHM pulse length, we can check if the beam is too much dispersed because of the beamsplitter:

$$\tau_1^{FWHM}(x) = \sqrt{1 + \frac{16\ln^2(2)GDD^2x^2}{(\tau_0^{FWHM})^4}} \quad (5.1)$$

We only do not know the value of GDD (Group Delay Dispersion), but we can get it from the next table taht shows values of different properties of the propagation of the light through a fused silica optic, the material of beamsplitters and most of the optics that we are going to use.

Material	$\Lambda$ (nm)	n ( $\lambda$ )	$dn/d\Lambda$ ( $\mu\text{m}^{-2}$ )	$d^2n/d\Lambda^2$ ( $\mu\text{m}^{-2}$ )	$d^3n/d\Lambda^3$ ( $\mu\text{m}^{-3}$ )	GVD ( $\text{fs}^2/\text{mm}$ )	TOD ( $\text{fs}^3/\text{mm}$ )
<b>Fused Silica</b>							
	400	1.470	-0.109	0.861	-9.600	97.43	30.2
	450	1.466	-0.076	0.512	-4.984	82.43	27.24
	500	1.462	-0.055	0.323	-2.809	71.4	25.53
	550	1.460	-0.042	0.214	-1.686	62.82	24.62
	600	1.458	-0.033	0.146	-1.064	55.85	24.28
	650	1.457	-0.027	0.103	-0.699	49.98	24.42
	700	1.455	-0.023	0.074	-0.476	44.87	24.99
	750	1.454	-0.020	0.054	-0.333	40.3	25.99
	800	1.453	-0.017	0.040	-0.239	36.11	27.44
	850	1.453	-0.016	0.030	-0.175	32.18	29.36

Figure 5.7: The dispersive properties of Fused Silica [18]

We can get GDD from GVD (Group Delay Dispersion) for a wavelength of 800 nm (our beam's wavelength) as:

$$GDD = GVD \cdot x$$

$$GDD = 36.1 \cdot 4.2624(\text{fs}^2\text{mm}/\text{mm})$$

$$GDD = 53.2(\text{fs}^2)$$

and knowing that our FWHM pulse length is  $\tau_0^{FWHM} \approx 125(\text{fs})$ , the equation 5.1 gives us a result of:

$$\tau_1^{FWHM}(4.2624(\text{mm})) = 125.04618(\text{fs}) \quad (5.2)$$

So, in the case that our beam has to go through some beamsplitters they won't add too much dispersion to the beam. It is important to discard things that can add an important dispersion to the final FROG trace, since we will see that the beam, before get the spectrum, has to pass through several optics and reflecting itself over several mirrors.

So now, we are ready to go into the FROG device except for one thing. We need to check that the polarization is the correct at the entrance of the FROG device. I had several problems because of the polarization, since the Newport approach for assembling the FROG device, need to have a horizontal polarization at the entrance of the spectrometer, and our Ti:Sapphire offers a vertical polarization. So we need to change the polarization, and we can change it with a  $\lambda/2$  wave-plate (WP). It is important to take care about the location of the wave-plate, it does not work in any place inside the FROG, we should put it before the FROG's pellicle beamsplitter (Pell), and that is at the entrance of the FROG setup.

By rotating the wave-plate and driving the beam through it and after, through a polarizing cube beamsplitter, I could get it.

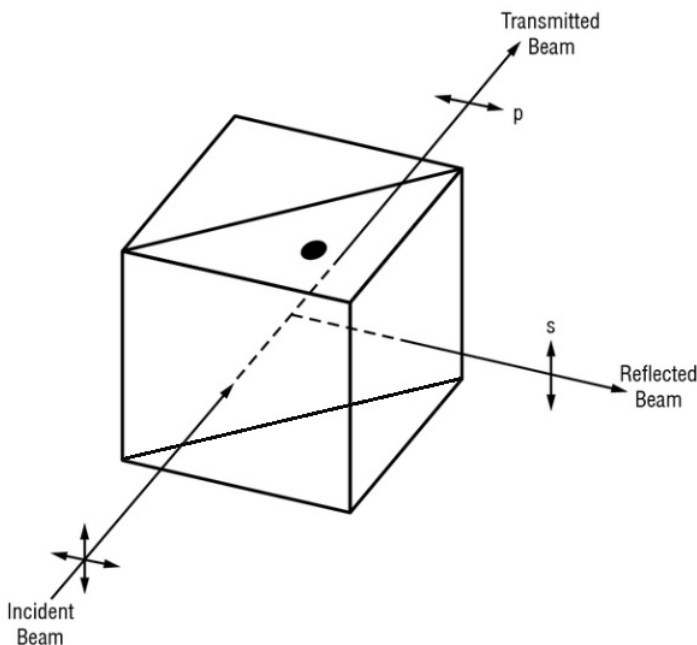


Figure 5.8: Polarizing Cube

So, let us go into the FROG device. Firstly we are going to put an iris assembly (IA1), that will help us to make sure that the input beam goes straight. Then, the beam goes through our 50%/50% pellicle beamsplitter (Pell). So, the beam is divided in two arms which go to the delay lines (DL1 and DL2).

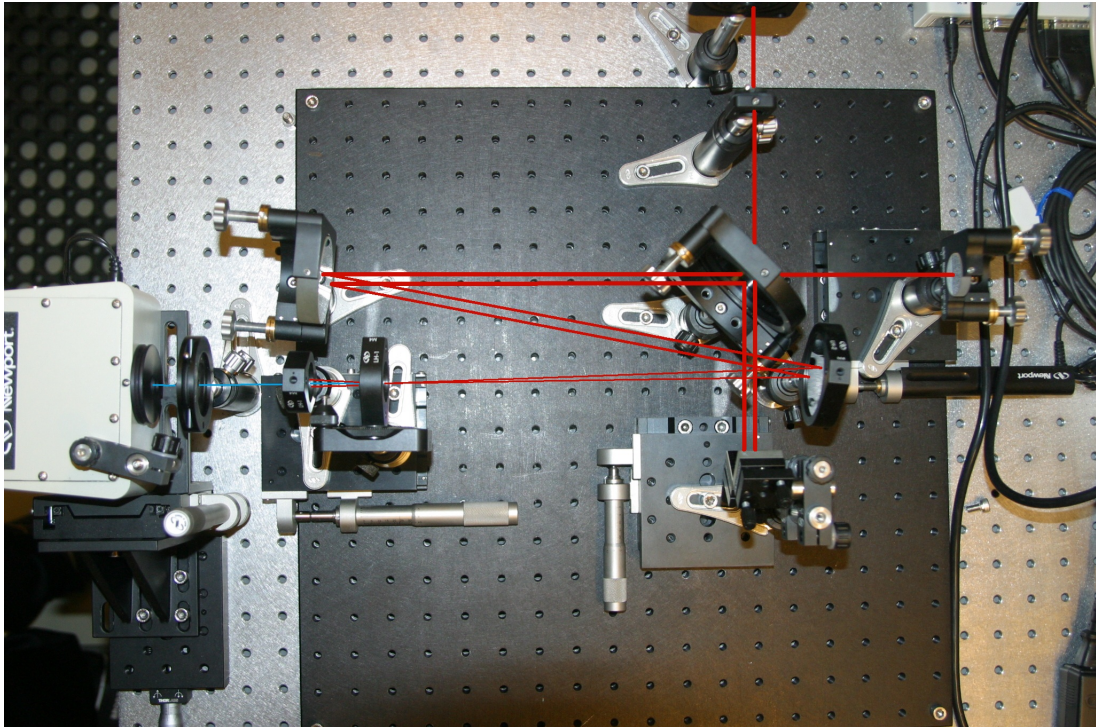


Figure 5.9: SHG FROG Device

With the delay line 1 we achieve to have separated and parallel both arms, approximately 2.5 (cm). With the delay line 2, which is controlled by the computer software sends its beam arm back to go through the pellicle. Both mirrors over the delay lines have to be separated from the pellicle at the same distance, roughly 11.5 (cm). The delay line 2 should be placed at least 200(mm) behind the wave-plate at the input of the device.

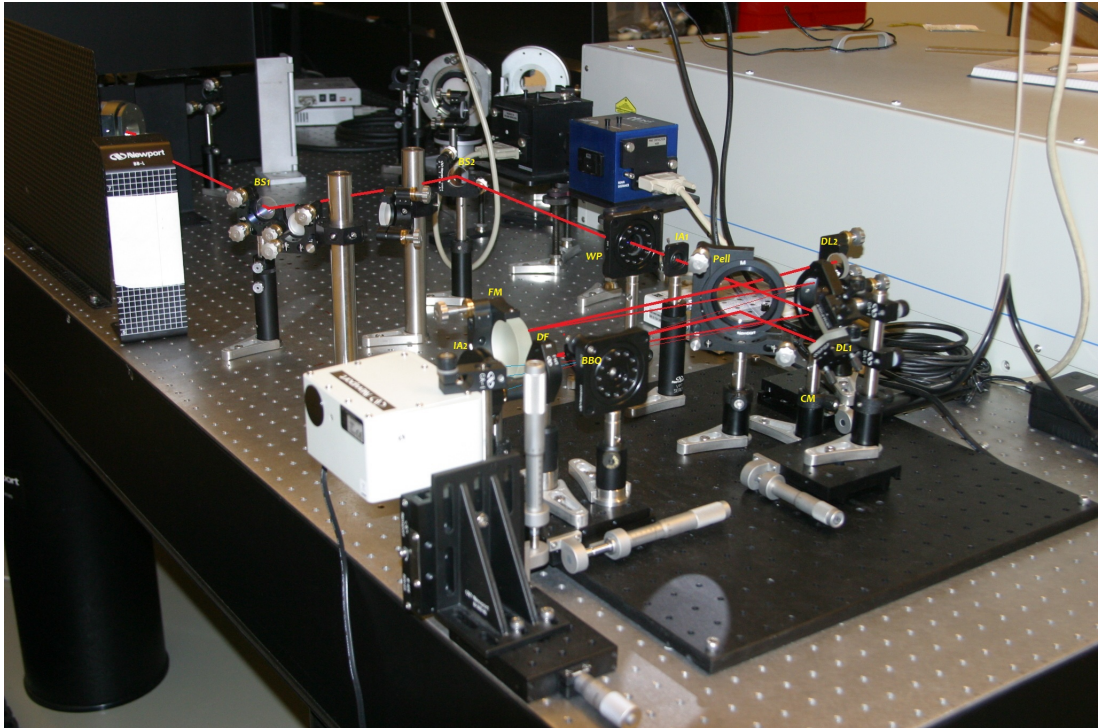


Figure 5.10: SHG FROG Device

After that both arms go parallel respect to each other towards the folding mirror (FM), which should be located 250 (mm) after the pellicle. Then, the arm goes to the focusing (concave) mirror (CM). From this mirror both arms are gonna be focused/overlapped in the middle point at BBO crystal, at 250 (mm) from the concave mirror.

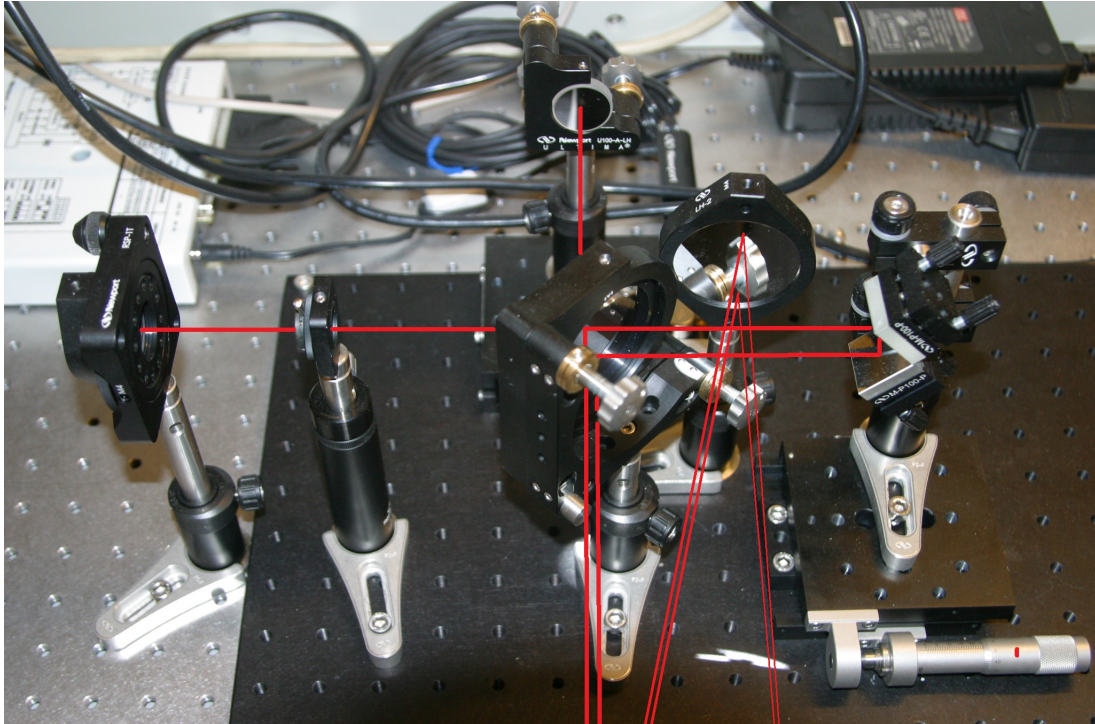


Figure 5.11: SHG FROG Device

Then, we have to rotate the nonlinear crystal (BBO) until finding one second-harmonic corresponding to one of the two arms, and noting the angle. Then, we have to go on until finding the second-harmonic corresponding to the other arm, and then noting the angle. Our SHG FROG beam appears when we put the nonlinear crystal at the middle angle between the two noted before.

The second-harmonic beams (blue) go through the dichroic filter (DF), and the fundamental beam (red) cannot pass through the filter. After that and close to the spectrometer entrance, we put a iris assembly (IA2), in order to get inside the spectrometer the SHG FROG and not the others second-harmonic beams.

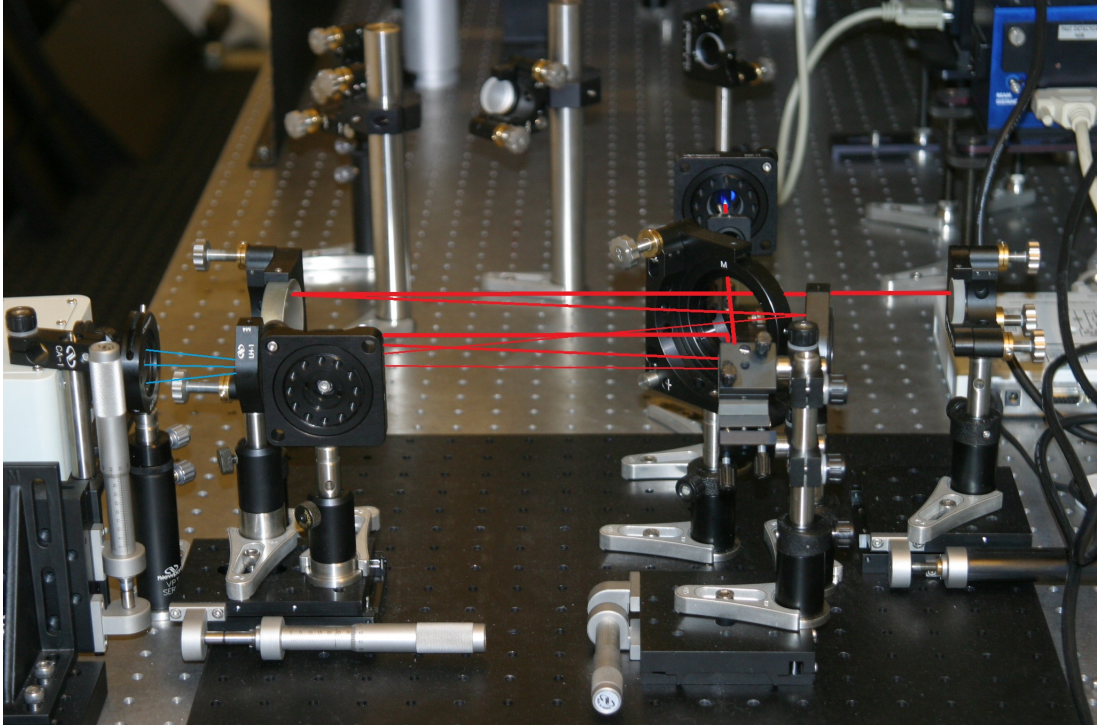


Figure 5.12: SHG FROG Device

So, that is all about the assembling of SHG FROG device. It is so important to check the polarization before starting to build the FROG device, it helps you to save much time. It is also important to make sure that the arms go parallel respect to each other after the delay line 1, as well as taking care about the distance between the optics.

## Chapter 6

# Measurements and analysis of FROG traces

### 6.1 Newport FROG Software

Once we have set up the FROG, we have to get the FROG trace from the spectrum with a specific software. This software manages the spectrometer detector and the motion stage that moves the delay line 2, in order to overlap both arms to achieve the SHG beam, being this movement time-dependent.

This software is so important, I would even say that it is critical for getting a good enough pulse from the spectrometer detector. Indeed, I had to use eighth versions of this software until get a newer version than the newest version, since I was dealing with a Newport technical supporter that was improving the newest version according I asked him for some issues related with the software perform. One of the principal problems was about the spectrometer calibration, since I could not exactly get the 800 *nm* pulse, value that I was supposed to have for the fundamental beam from the Ti:Sapphire laser. It is so important to take in account because the pulse could not appear completely centered in 800 nm in the software screen, and improving the calibration could mean a better pulse measured and showed in the software.

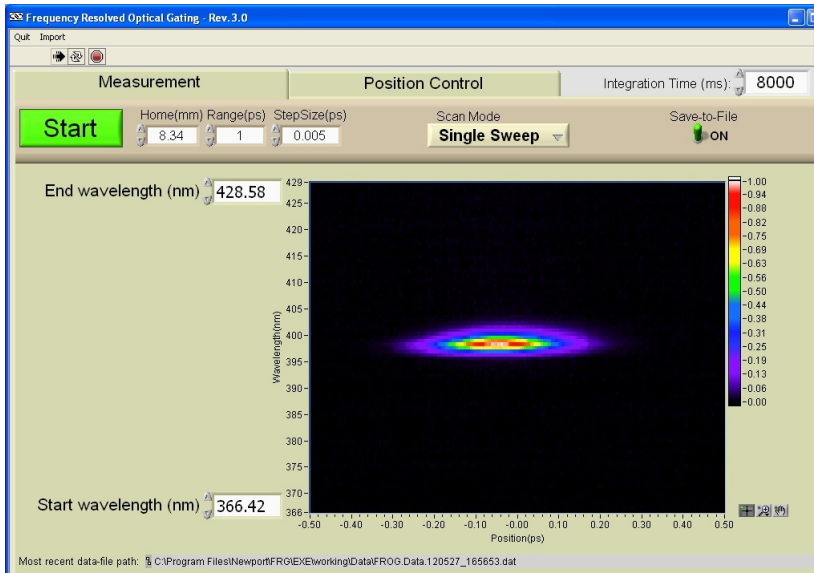


Figure 6.1: Screenshot of FROG software of Newport

By managing the integration time, step size in time, wavelength range and time-domain range we can obtain our FROG trace. The trace that we obtain here can be analyzed by the software from Femtotech, FROG 3.2.0. We are going to deal with that software at the next section.

## 6.2 Femtotech FROG 3.2.0. Software

So, we have our FROG traces, after a hard work carried out at the laboratory about aligning optics during several weeks, some problems with the performance of the FROG-traces-scanning, calibrating the spectrometer...etc. And now what? What is next?

Well, we are ready to retrieve the phase and intensity in time-domain and frequency-domain by means of the FROG 3.2.0. software, which uses a FROG algorithm in order to retrieve the pulse from the trace with a minimum error rate. This error is the *FROG error*, and is the difference existing between the original FROG trace that we have obtained from the minispectrometer and the retrieved trace, obtained from this software. We need to achieve the convergence of the algorithm to an error value smaller than 1%, which would be a good convergence of course, but we are gonna try to go down 0.5%.

The typical values for FROG errors achieved in experiments are given by the FROG's inventor, Rick Trebino [6]. With arrays (grids) of 128 x 128, and a BBO crystal thickness of no more than 100  $\mu\text{m}$  for measuring 100 femtoseconds (800 nanometers) pulses using SHG FROG, the error should be  $< 0.5\%$ [20]. Errors tend to be lower for larger arrays because, due to Fast Fourier Transform relations between the delay and frequency axis ranges increment, the fractional area of the trace that is nonzero is less in the larger array traces.

It has to be said that in this chapter I am not going to do an extensive explanation about how this software works, I will do that at the end of this paper, in Appendix B. Anyway, here I leave a screenshot where we can see the original pulse measured, the retrieved trace and its temporal and spectral properties such the phase and intensity.

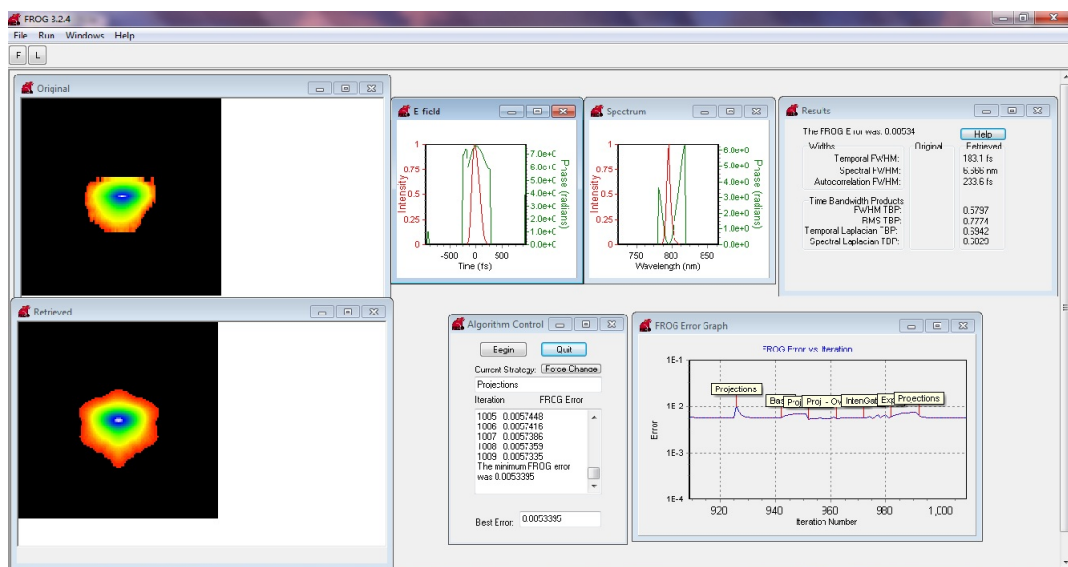


Figure 6.2: Screenshot of FROG software Femtosoft

We can also see how the algorithm has worked as well as some dispersive parameters obtained from this analysis of the FROG trace.

### 6.3 Characterization of our pulse of reference

At the output of our Ti:Sapphire laser we have a beam of a fixed wavelength of  $800\text{ nm}$ , with a *Full-Width Half-Maximum* around of  $125\text{ fs}$  and a power output of  $400\text{ mW}$ .

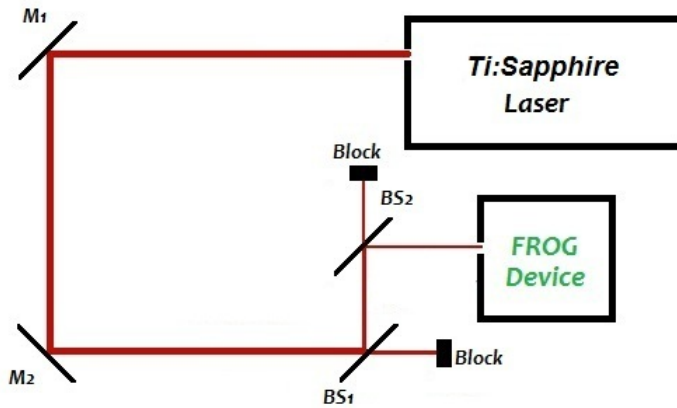


Figure 6.3: Set up to measure the pulse of reference

After several reflections over every mirror, beamsplitter or another kind of optics, the beam will appear positively chirped at the end of the beam path, and we will check that with the spectrometer.

For this first measure we chose the next parameters:

*In Newport's software*

Delay range  $\Rightarrow -500\text{fs} \leq \tau \leq 500\text{fs}$

Delay Step size  $\Rightarrow \Delta\tau = 10\text{fs}$

Wavelength Step size  $\Rightarrow \Delta\lambda = 0.6581\text{nm}$ , fixed by the spectrometer.

Wavelength range  $\Rightarrow 366.42\text{nm} \leq \lambda \leq 428.58\text{nm}$

*In Femtosoftware's software*

Grid size  $\Rightarrow N = 128$

Order  $\Rightarrow$  Delay

Read in as  $\Rightarrow$  ConstantWavelength

Wavelength Centering  $\Rightarrow$  Peak

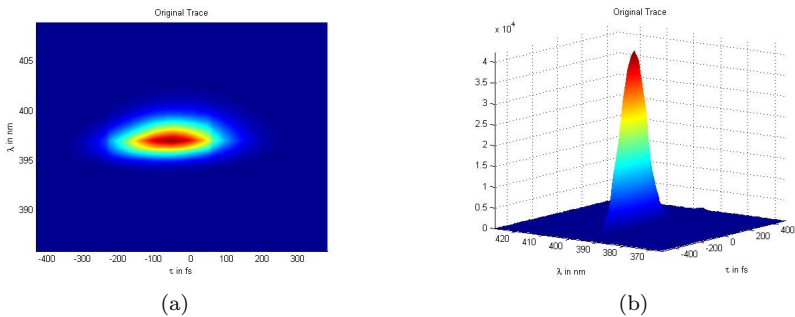


Figure 6.4: FROG trace of the reference pulse

Above we can see the trace obtained with the FROG (Newport) software, and plotted using matlab. The code for plotting this trace and all the next figures, appears in *Appendix C* at the end of this paper. Some of that code was taken from Martin Jackisch's work [4].

In the picture below we can see both the original and the retrieved pulse given by FROG 3.2.0. software (Femtosoft). We can note that this pictures are narrower than the FROG trace, what is logic, since we have obtained that trace by an autocorrelation of the original pulse, and then, integrating in time.

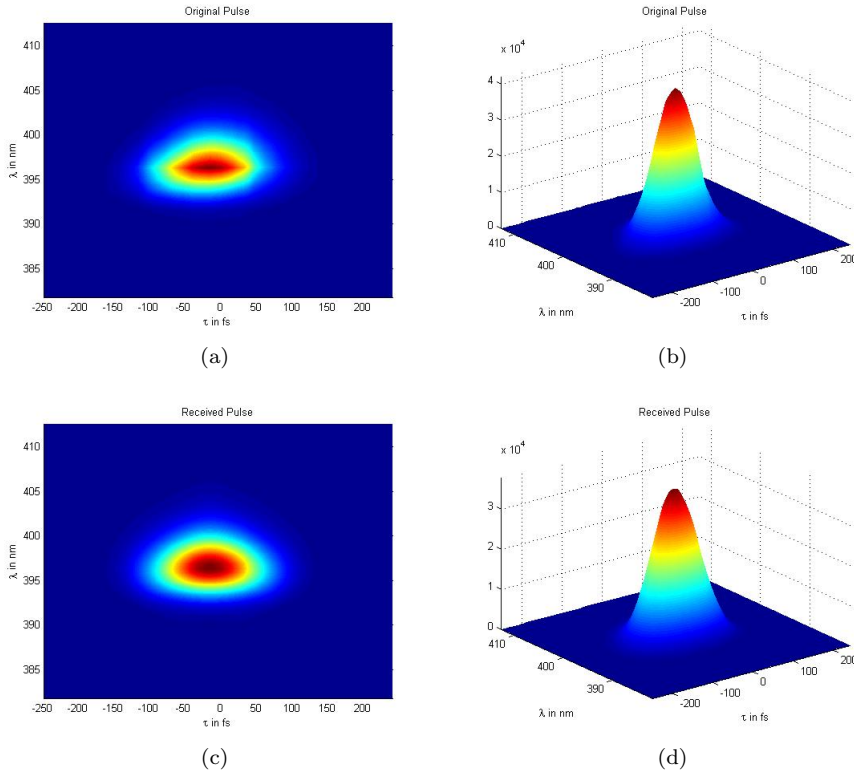
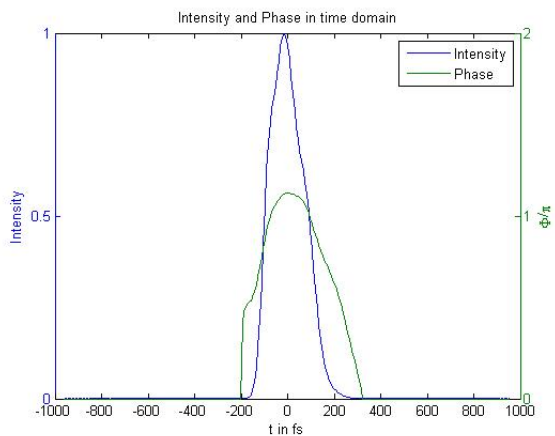
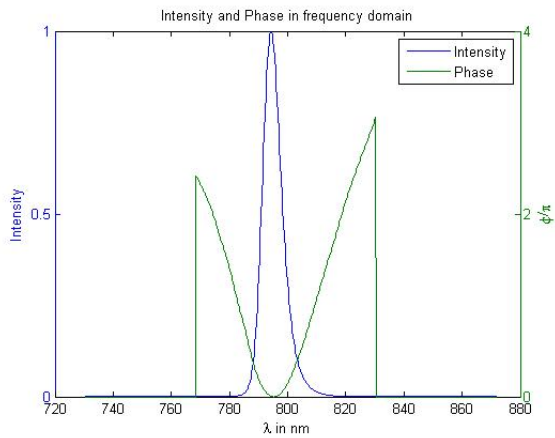


Figure 6.5: Original Pulse (a)(b) and Retrieved pulse (c)(d)

We can check in the next figures that the our FROG trace really corresponds to a positively chirped SHG FROG trace, as it had been said, commonly happened because of the path followed by the fundamental beam, going through some optics and reflecting in others.



(a)



(b)

Figure 6.6: Retrieved electric field from the reference pulse in (a) time domain and (b) frequency domain

We can check that with the table above of comparison of traces for common ultrashort pulse distortions for the most common FROG beam geometries given by the inventor of FROG, Rick Trebino [20].

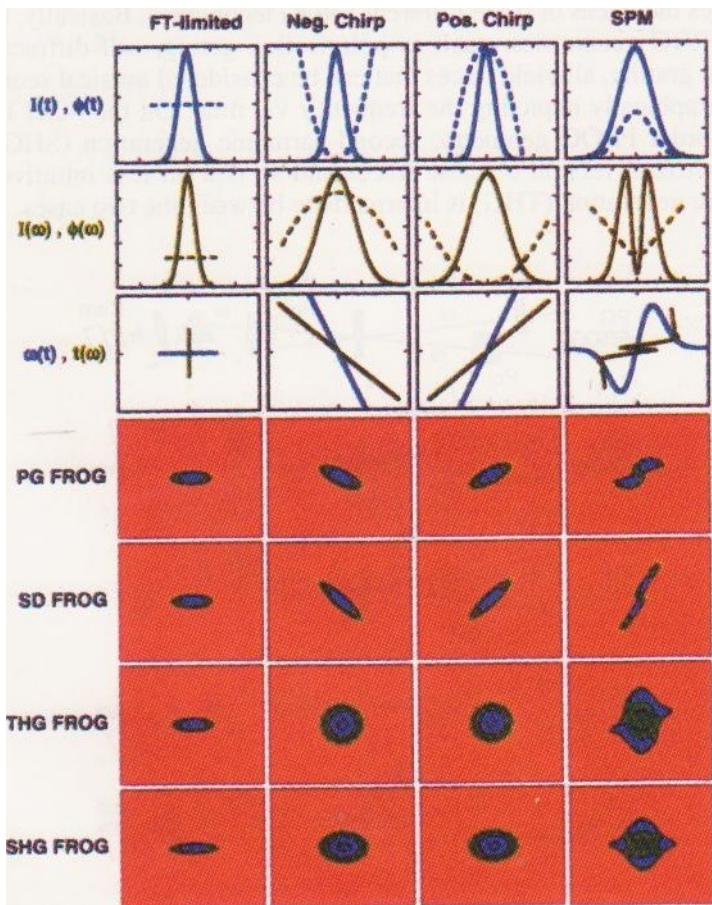


Figure 6.7: Comparison of FROG beam geometries

So that is fine, it seems that we have obtained, at least qualitatively, a correct SHG FROG trace from our optics setup. But, what about the FROG algorithm error value? We have to remind, as it has been said some paragraphs above, that we should get a value down to 0.5% for a SHG frog after using a 128 x 128 grid in Femtosoftware's software.

But we were so close but not down, we got a algorithm error of 0.56994%, which is not a bad result, since a good FROG algorithm error must be down 1% and it is. Obviously, when we took a larger grid, we got error values down 0.5%, as occurs in every Fourier Transform operation, the more N (grid) points taken, the more precise results obtained. However it also occurs paralelly that, the more N points taken, the bigger computing cost.

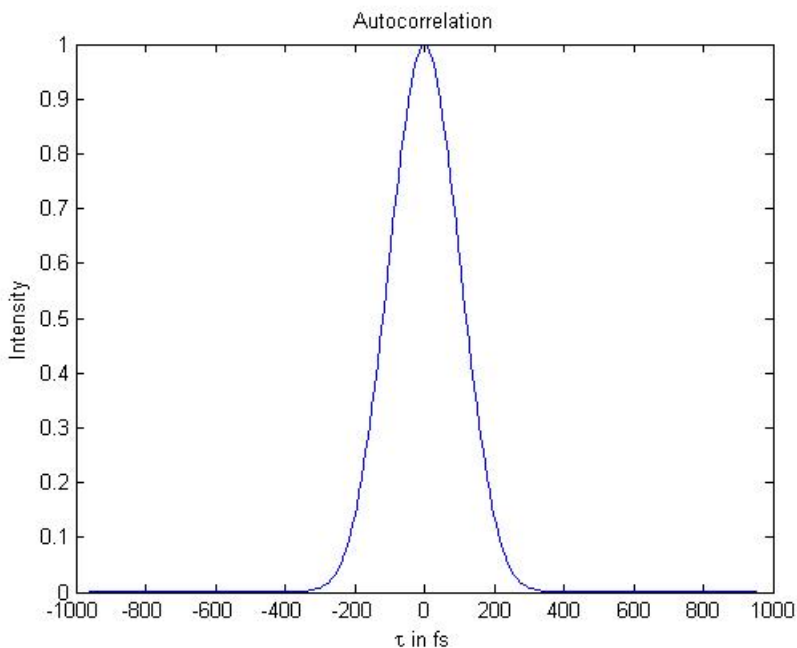


Figure 6.8: Autocorrelation of the reference pulse

We should remind that the FROG error that we are using concerns the difference between the original pulse and the retrieved pulse, and many systematic errors could have made during the assembling of the FROG setup device, one or several of them could add an extra delay to the original pulse. It could be, for that reason, we obtained from the analisis software (Femtosoftware) a *FWHM* value of 190 fs, that is 65 fs more than the 125 fs from the original beam of Ti:Sapphire laser.

As we have said, many factors could affect the beam. One of the most important could be the phase matching [6], a nonlinear effect that talk about the correct coincidence of the two arms into the nonlinear BBO crystal, inside the FROG setup. Since a very small error in phase matching could shift the pulse from the

center at the time axis. In fact, every time I took off the BBO from the FROG device and then put it again, the pulse *FWHM*, varied slightly.

But more errors could have been made to obtain some times a pulse *FWHM* around 170 *fs* and others, 190 *fs*. In Trebino's book [6] there is a entire chapter about the most common errors made in the assembling of a FROG setup. I have listed below some practical factors to take in account:

- Trebino says in his book that for a 100 *fs* pulse is necessary to use a BBO with a thickness of no more than 100  $\mu m$  . And I used a 100  $\mu m$  crystal for a 125 *fs* pulse.

- The different optics that I used, have the spectrometer resolution, and some aligning problem could have been bothering the beam all the time. Even the integration time that I used in the Newport's FROG software, could have been too high. But I had to take a very high integration time because of the second harmonic was too hard to detect with lower values of integration time.

- The Minispectrometer could have not been completely calibrated, since I finally got a 795  $\mu m$  fundamental beam, 397.5  $\mu m$  SHG, and not 800  $\mu m$  (400  $\mu m$  SHG) as hoped.

Anyway, I could check succesfully the dispersion effect of the water over the pulse in different experiments whose results we are gonna see in the next sections.

## 6.4 Increasing chirp effect

### 6.4.1 10 mm Water cuvette

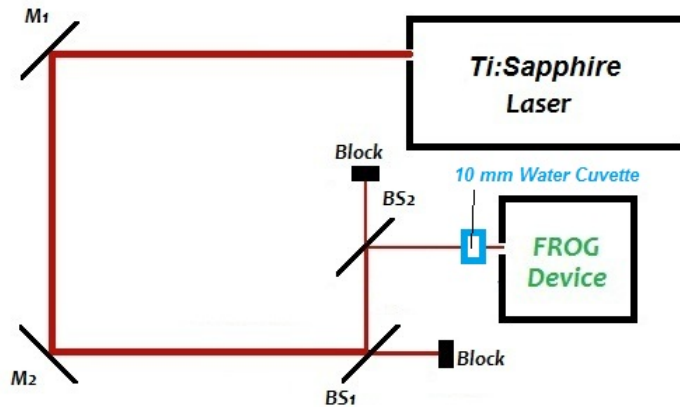


Figure 6.9: Set up including a water cuvette of 10 mm

In the picture above we see that a new stuff was included in our setup between the fundamental beam and the FROG setup, a 10 mm cuvette filled with tap water.

We can note that the chirp effect was slightly increased in the graphs below:

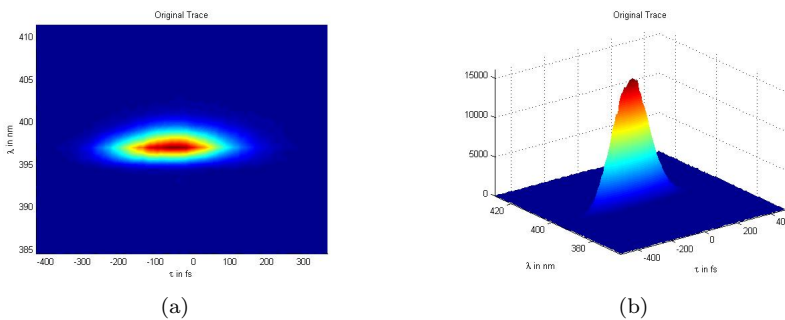


Figure 6.10: FROG trace with 10 mm water cuvette

Although is a bit hard to note, the pulse FWHM is bigger than the reference

pulse, because of the effect of water. We have obtained now a value of 198.11 fs for the pulse FWHM.

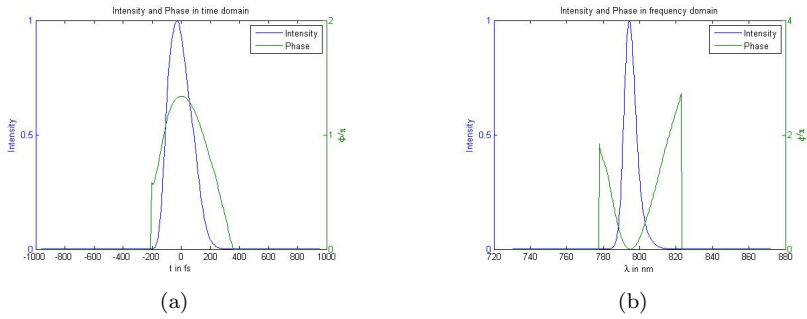


Figure 6.11: Retrieved electric field from the reference pulse in (a) time domain and (b) frequency domain

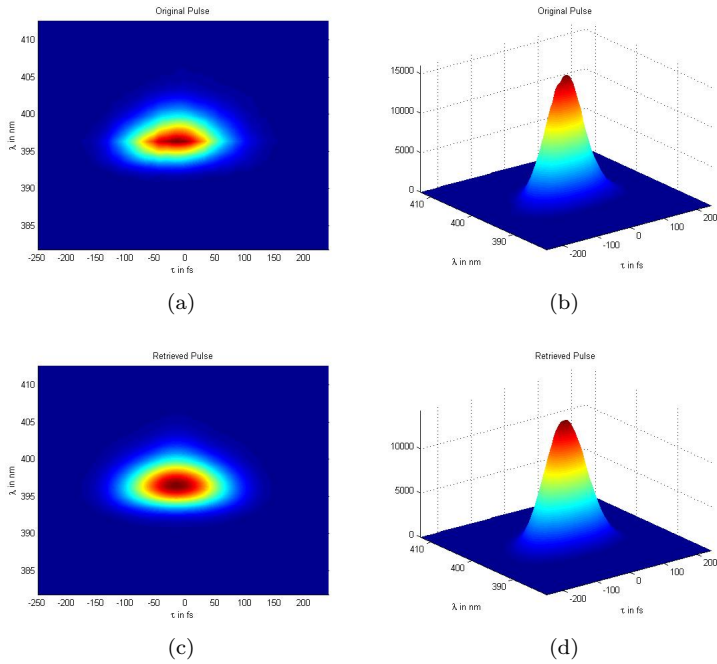


Figure 6.12: Original Pulse (a)(b) and Retrieved pulse (c)(d)

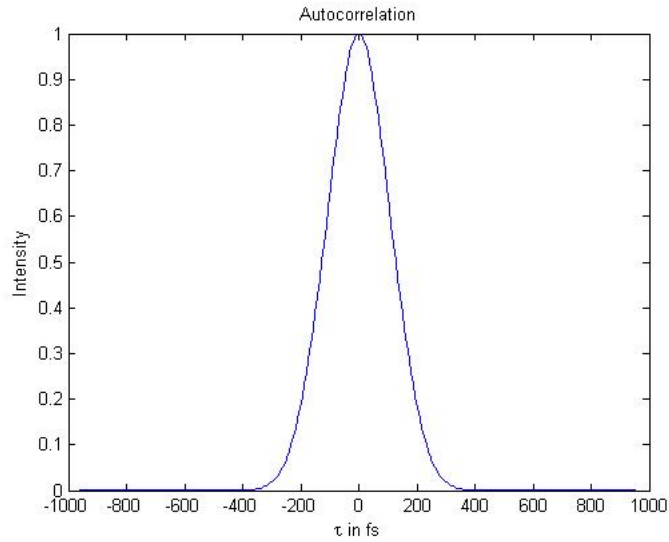


Figure 6.13: Autocorrelation of the reference pulse

If the pulse is wider, the autocorrelation too. For the reference pulse we had a value of  $239.59$  fs for the autocorrelation and now we have  $255.42$  fs. Furthermore, the FROG error algorithm minimum value obtained is  $0.56172\%$ , slightly higher than the reference pulse FROG error.

### 6.4.2 50 mm Water cuvette

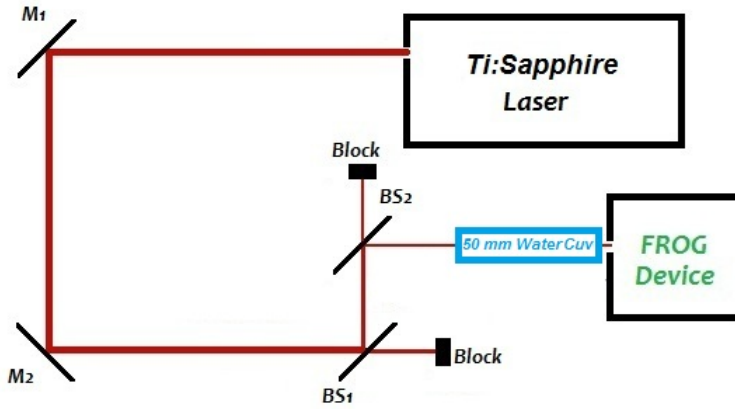


Figure 6.14: Set up including a water cuvette of 50 mm

Now, we have included a 50 mm cuvette filled with tap water and we can not that the chirp effect go on increasing.

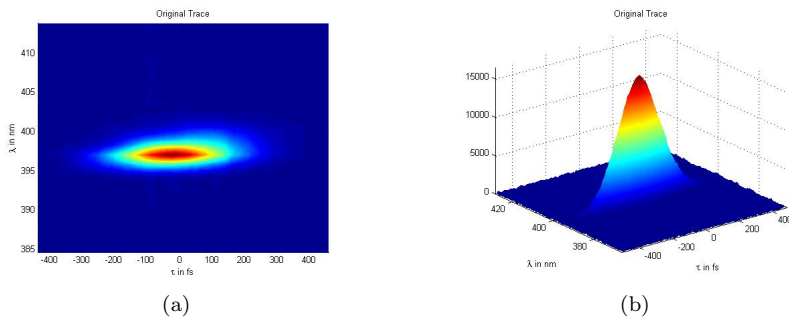


Figure 6.15: FROG trace with a 50 mm cuvette included

The pulse FWHM is now 247.81 fs.

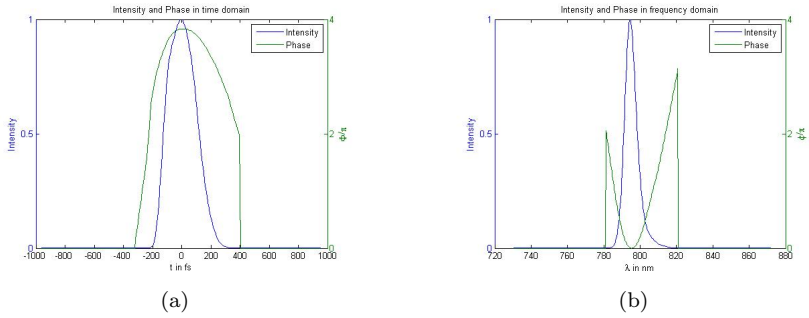


Figure 6.16: Retrieved electric field with a 50 mm cuvette included in (a) time domain and (b) frequency domain

The FROG algorithm error minimum value obtained also increases in this case, going over 1%.

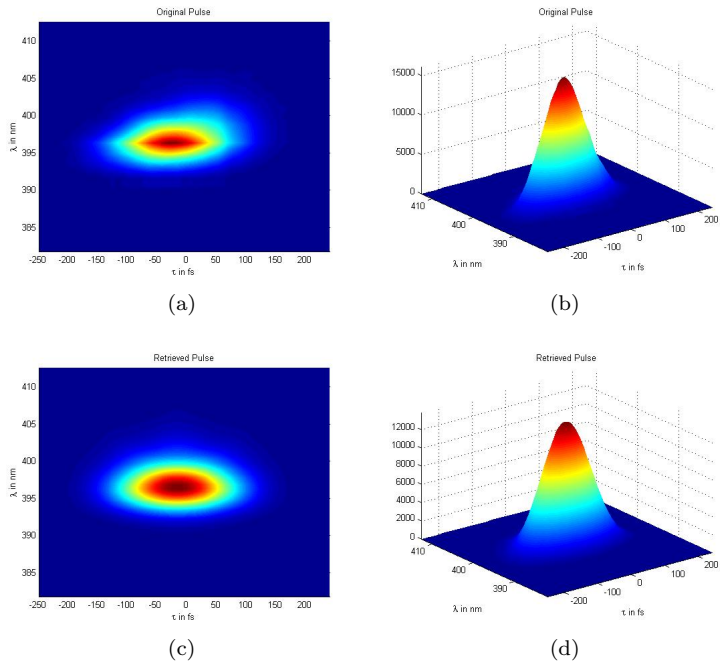


Figure 6.17: Original Pulse (a)(b) and Retrieved pulse (c)(d)

The autocorrelation is even wider now than before, 311.05 fs.

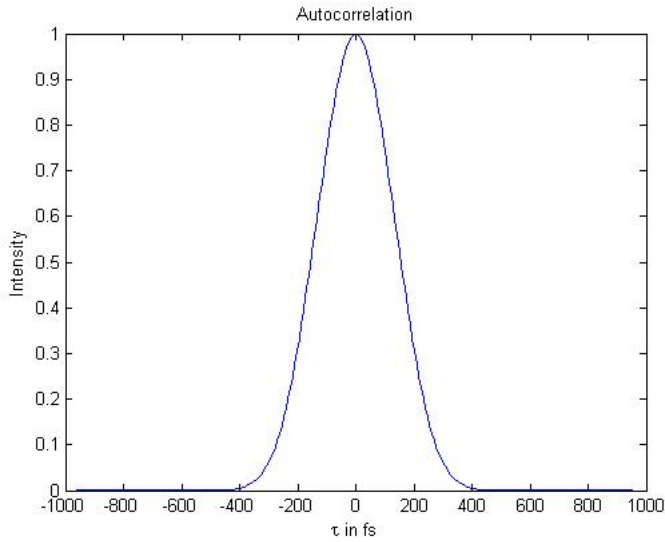


Figure 6.18: Autocorrelation with a 50 mm cuvette included

### 6.4.3 100 mm Water cuvette

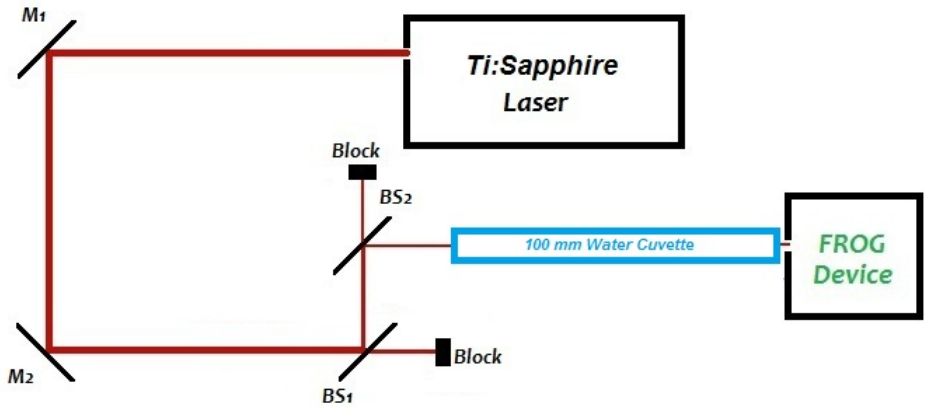


Figure 6.19: Set up including a water cuvette of 100 mm

Now we are gonna use the largest cuvette that we had, a 100 mm cuvette, also filled with tap water.

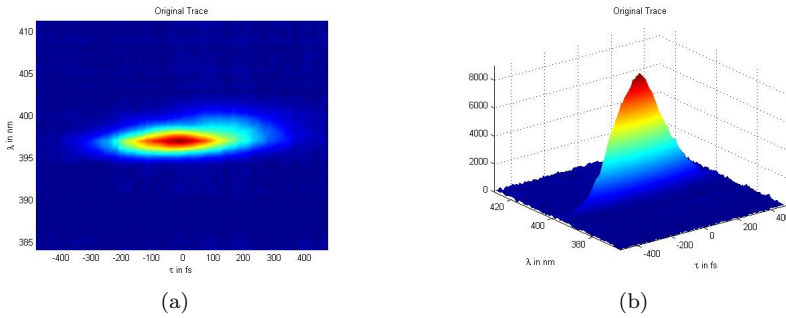


Figure 6.20: FROG trace with a 100 mm cuvette included

The pulse FWHM is now 319.69 fs.

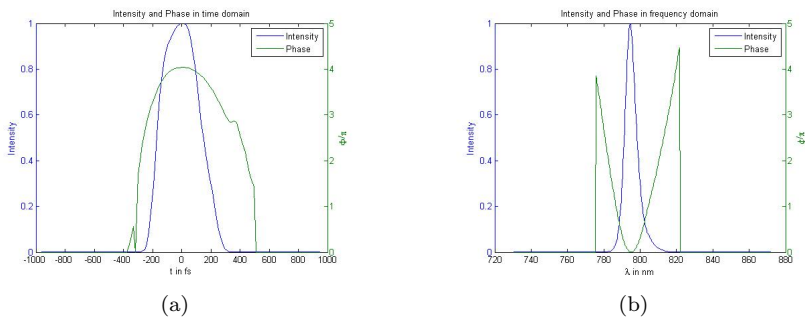


Figure 6.21: Retrieved electric field a 100 mm cuvette included in (a) time domain and (b) frequency domain

The FROG algorithm error minimum value obtained also increases in this case, going over 1.5418%.

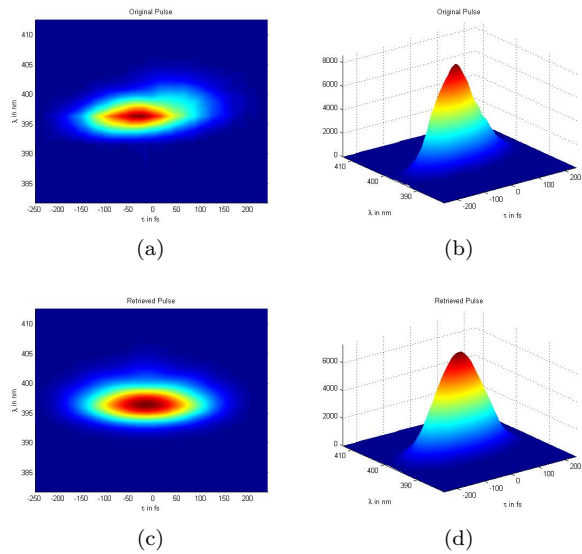


Figure 6.22: Original Pulse (a)(b) and Retrieved pulse (c)(d)

The autocorrelation is even wider now than before, 393.63 fs.

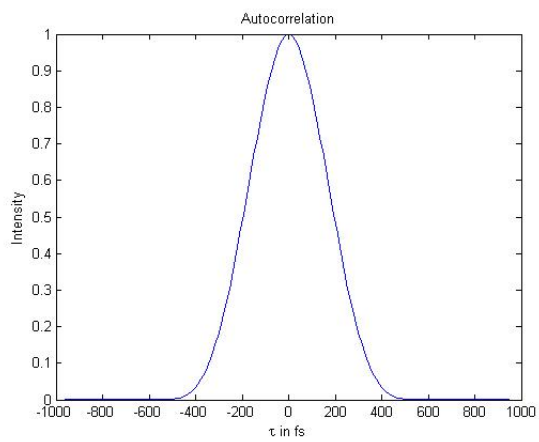


Figure 6.23: Autocorrelation a 100 mm cuvette included

Now it would be interesting to see how the spectral phase is changing according to the chirp effect is increased.

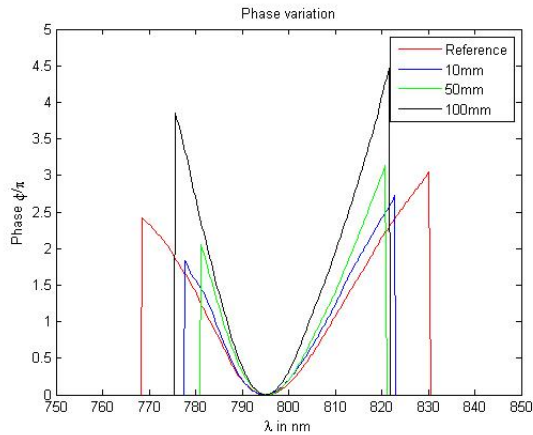


Figure 6.24: Comparison of the spectral phases

We can also see how the chirp effect increases the autocorrelation, the larger cuvette the wider autocorrelation.

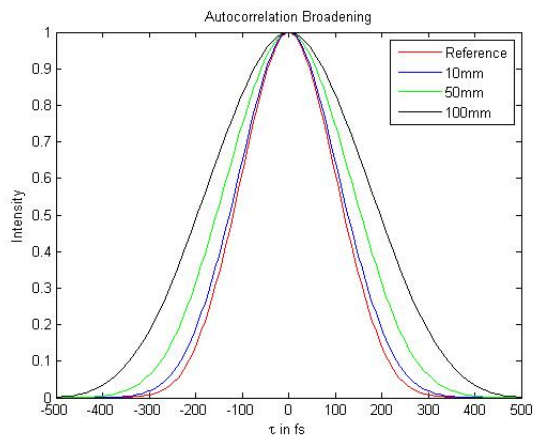


Figure 6.25: Comparison of the autocorrelations

# Chapter 7

## Conclusion

All this work goes around the necessity of characterizing an ultrashort pulse in order to use it in measurements of very very short events.

The problem is that we have to characterize an unknown event, the shortest event ever created, the ultrashort pulse. And we cannot use any method to do that, we need to use the Frequency-Resolved Optical-Gating. We have seen that the previous techniques or methods used to measure an ultrashort pulse, could not achieve a complete success.

In time-domain we had the *Intensity autocorrelation* that provided the pulse field but not the phase, while in frequency-domain we had the spectrum, which also could not characterize an unknown ultrashort pulse completely.

So, at the end of this work our goal was to be able of characterizing an ultrashort laser pulse with the *Frequency-Resolved Optical-Gating* method, and we have achieved that.

Despite of the extra delay obtained in the characterization of such pulse, because of the different systematic errors that could have been made during either the assembling of the FROG device setup or the beam path from the Ti:Sapphire laser until the entrance of the FROG device. It also might have occurred some measurement error with one of the different softwares used in these experiments or the calibration of the spectrometer may have influenced in the final results.

We have obtained a good enough FROG algorithm error value, down the 1% demanded and around 0.5% hoped for a SHG FROG measurement with a 128 x 128 grid.

We also could see the dispersive effect of the water over the pulse, adding a positive

chirp effect, showing us one of the several possibilities that offers this ultrashort pulse measuring technique. An almost perfect chirp can provide us a different spectral component of a pulse in different instants of time, and it is so useful for the scientific areas that work with a very short events.

We have seen that, the longer water cuvette placed between the beam and the FROG device, the more chirped pulse achieved.

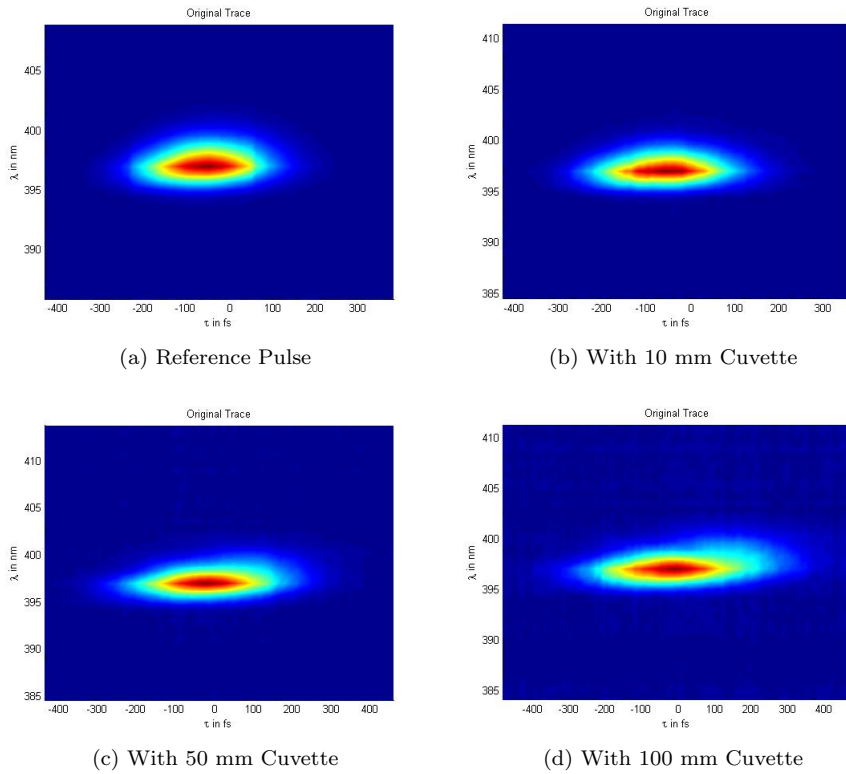


Figure 7.1: Evolution of the chirp effect using different water cuvette lengths

## 7.1 Future work

One of the several things, and more interesting, that could be made from this work would be to send an ultrashort pulse through a portion of optic fiber and then, check the dispersion effect of the glass fiber over the pulse.

Maybe, before doing a measurement with the optic fiber, would be interesting to improve the FROG device and the measurements made in this work, in order to get a better FWHM value in the characterization of the reference pulse.

In order to do a better measurement it would be nice to use the marginal value from the spectrum of the fundamental beam and comparing it with the marginal file generated by the Femtosoft FROG 3.2.0 software belongin to the FROG trace measured by the Newport's software. I tried it, because it is supposed that by using the marginals correction you can achieve a better relationship between the original pulse and the retrieved pulse, and that means, a better FROG algorithm error value. But I could not obtain a better result using the marginals property, but worse.

It would be interesting to do some little changes on the setup to perform another of the FROG beam geometries, as the Self-Diffraction (SD) FROG, and take some measurements to compare with the SHG FROG results.

# Chapter 8

## Summary

Communication technologies are continuously evolving since were invented the telegraph. Nowadays, one of the most interesting and relatively youngest field of telecommunications are the optical communications. The search of the shortest event ever created to measure very fast/short events is now possible because of the *Light Amplification by Stimulated Emission of Radiation*, longer known as *laser*.

So well, we need to find the shortest event but we need to know how to measure it, since it is supposed that there is not a shorter event. So we need the pulse to measure itself, and its sound as we need to do a kind of autocorrelation.

In order to measure a pulse, we need to get its intensity and phase in either the time or frequency domains. And, before the FROG appearance, it was done with autocorrelation (time-domain) and spectrum (frequency-domain).

And that was one of the firsts techniques used to characterize an ultrashort laser pulse, called the *Intensity Autocorrelation*. The intensity autocorrelation results when a pulse is used to measure itself in the time domain.

Firstly, the pulse is splitting into two arms, after that one of them is delayed respect the other one. Finally we have to overlap both arms spatially in a nonlinear-optical medium such a second-harmonic generation crystal(SHG).

$$A^{(2)}(\tau) = \int_{-\infty}^{+\infty} I(t + \tau)I(t)dt \quad (8.1)$$

The target in the frequency domain is the spectrum. There are some devices that can get the spectrum, they are the spectrometer and the interferometer. There are

several ways to perform a spectrometer either diffraction-grating device or Fourier-transform spectrometers.

The last ones operate in the time domain and measure the transmitted integrated intensity from a Michelson interferometer, often called the light's second-order coherence function, also called the interferogram and the field autocorrelation:

$$\Gamma^{(2)}(\tau) = \int_{-\infty}^{+\infty} E(t)E^*(t - \tau)dt \quad (8.2)$$

And its Fourier transform gives the spectrum, the Autocorrelation Theorem:

$$|\tilde{E}(\omega)|^2 = \text{F} \left\{ \int_{-\infty}^{+\infty} E(t)E^*(t - \tau)dt \right\} \quad (8.3)$$

We have seen that we can get the spectrum, but just this, the spectrum. We cannot get the spectral phase easily, since there are too many pulses that correspond to a given spectrum. We are dealing then with a one-dimensional phase-retrieval problem, since we want to retrieve the spectral phase from the spectrum using additional information, and this kind of problem is usually unsolvable.

Summarizing, maybe the autocorrelation and spectrum could not measure ultra-short pulses very well, but they have been the best results until better techniques were discovered or invented.

The *Frequency-Resolved Optical-Gating* appears to solve the problems that autocorrelation and spectrum could not, neither separately or both together. FROG measures a spectrogram of the pulse.

An example of a FROG trace could be:

$$I_{FROG}^{SHG}(\omega, \tau) = \left| \int_{-\infty}^{\infty} E(t)E(t - \tau)e^{-j\omega t}dt \right|^2. \quad (8.4)$$

Is interesting to see that the FROG trace is a spectrogram in which the pulse intensity gates itself where the gate function here is  $E(t - \tau)$ . In order to obtain  $E(t)$  from its FROG trace we have to consider that  $E_{sig}(t, \tau) \propto E(t)E(t - \tau)$  is considered as the Fourier transform with respect to  $\tau$ , of a new quantity called  $\bar{E}_{sig}(t, \Omega)$ :

$$E_{sig}(t, \tau) = \int_{-\infty}^{\infty} \overline{E}_{sig}(t, \Omega) e^{-j\Omega\tau} d\Omega \quad (8.5)$$

So, once we have found either  $E_{sig}(t, \tau)$  or  $\overline{E}_{sig}(t, \Omega)$  the pulse field  $E(t)$  is given. So, to find  $E(t)$  we just need to know  $\overline{E}_{sig}(t, \Omega)$ , then if we substituting the equation into the FROG trace we have:

$$I_{FROG}^{SHG}(\omega, \tau) = \left| \int_{-\infty}^{\infty} \int_{-\infty}^{\infty} \overline{E}_{sig}(t, \Omega) e^{-j\omega t - j\Omega\tau} dt d\Omega \right|^2. \quad (8.6)$$

This expression yields the magnitude, but not the phase. So the problem now is to find the phase of  $\overline{E}_{sig}(t, \Omega)$ , being know this inversion problem as the two-dimensional phase-retrieval problem.

The difference between the two-dimensional phase-retrieval problem and the one-dimensional phase-retrieval problem is that, the first one has, however, an unique solution and is a solved problem when certain additional information about  $\overline{E}_{sig}(t, \Omega)$  is available, while in the one-dimensional phase-retrieval problem many solutions can exist. The two-dimensional phase retrieval problem has only *trivial* ambiguities. Is too hard that another solution may exist, but it normally does not occur. Is important to say that using an iterative algorithm, the pulse field  $E(t)$  could be determined.

We have seen that the most important property of FROG is that we can get the pulse intensity and phase either estimating by looking at experimental FROG trace or using the iterative algorithm to retrieve the precise values of intensity and phase versus time or frequency.

FROG is highly accurate, especially for measuring the phase in the wings of the pulse. It is experimentally simple and very general, we can use FROG to measure simple and complex pulses. FROG can measure a wide range of pulse lengths, from a few femtoseconds to many picoseconds.

We can agree in the fact tha FROG is a powerful tool to measure ultrashort laser pulses, but there some aspects of intensity and phase that it cannot measure. FROG doesn't measure the absolute phase,  $\phi_0$  in the Taylor expansion of spectral phase, since it is a mag-squared magnitude. As the pulse is gating itself, there is no absolute time reference, so it cannot measure, for example, the arrival time,  $\phi_1$ , the firs-order term coefficient in the spectral-phase Taylor series.

## 8.1 Experimental work

My whole work in the laboratory goes around the SHG FROG, and as we saw in equation 4.1, it is based in a SHG autocorrelator, spectrally resolved.

The main advantage of SHG FROG is sensitivity, unlike the other geometries with SHG FROG we just have to deal with a only second-order nonlinearity. It is commonly used to measure unamplified pulses directly from a Ti:Shapphire oscillator, as I did.

SHG FROG also gives the best signal-to-noise ratios because of its different signal beam colour and it is also ideal for few-femtoseconds pulse measurement.

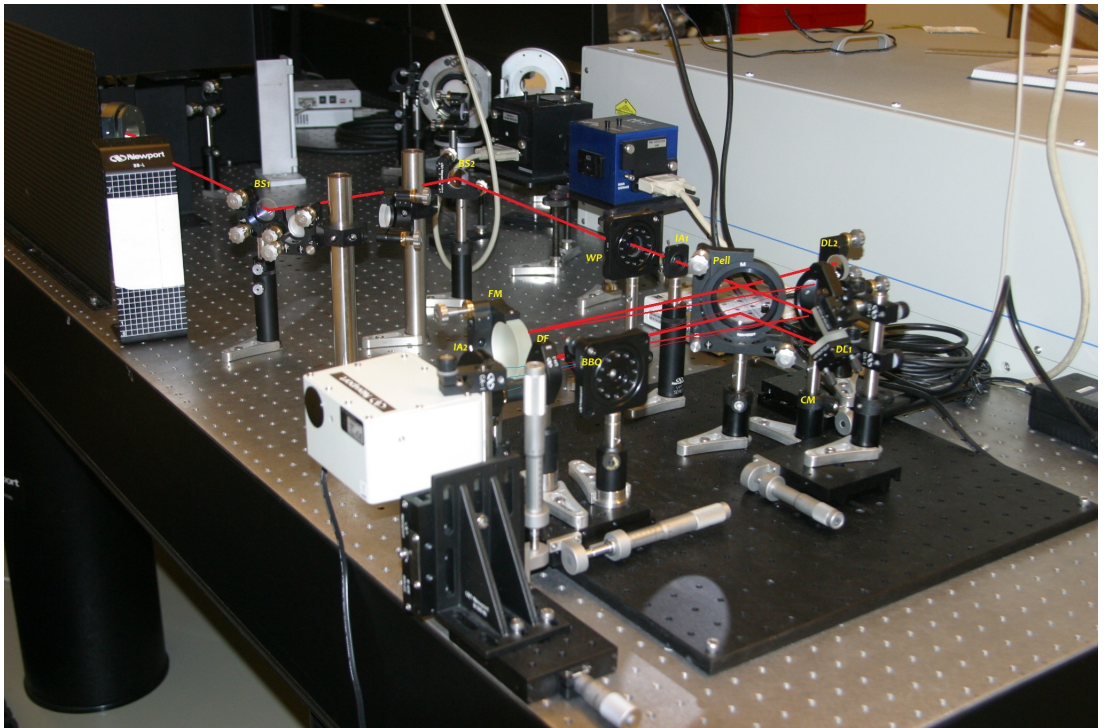
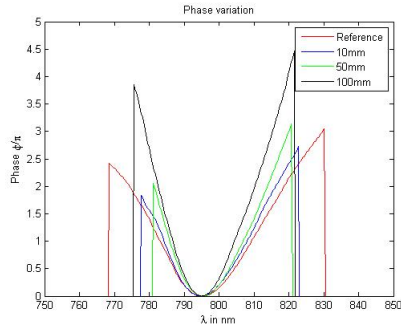


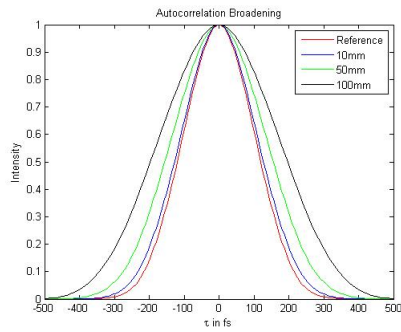
Figure 8.1: SHG FROG Device

We characterized the pulse, and then we checked how the chirp effect increase according to the length of some cuvettes placed between the beam and the FROG

setup. We could see how the spectral phase is changing according to the chirp effect is increased and how the chirp effect increases the autocorrelation value.



(a) Comparison of the spectral phases



(b) Comparison of the autocorrelations

Figure 8.2

So we could see experimentally how the dispersive effect of the water over the pulse, added a positive chirp effect, showing us one of the several possibilities that offers this ultrashort pulse measuring technique.

## References

- [1] Rick Trebino, et al., *Frequency-Resolved Optical Gating: The Measurement of Ultrashort Laser Pulses*. Kluwer Academic Publishers, Boston, p. 2, 2000 .
- [2] Daniel Fleisch, *A Student's Guide to Maxwell's Equations*. Cambridge University Press, 2008.
- [3] Harry Bateman, *The Mathematical Analysis of Electrical and Optical Wave-Motion on the Basis of Maxwell's Equations*. Forgotten Books, 2010.
- [4] Martin Jackisch, "Design and construction of a frequency-resolved optical gate using an autocorrelator and a high-resolution monochromator." Diploma Thesis, Darmouth College (USA) and Helmut Schmidt University (Hamburg), pp. 3-4, 2006.
- [5] Rick Trebino, et al., *Frequency-Resolved Optical Gating: The Measurement of Ultrashort Laser Pulses*. Kluwer Academic Publishers, Boston, p. 11, 2000.
- [6] Rick Trebino, et al., *Frequency-Resolved Optical Gating: The Measurement of Ultrashort Laser Pulses*. Kluwer Academic Publishers, Boston, 2000.
- [7] C. J. Hope and d. J. Furlong, *Time-Frequency distributions for timbre morphing: The Wigner distribution versus the stft*. Proceedings of the SBCMI, Brazil, August 1997. <http://www.ciaranhope.com/paper1.html>
- [8] J. Ville, *Theorie et applications de la notion de signal analytique*, Cables et Transmission, vol. 2A, 1948.
- [9] T.A.C.M. Claasen and W.F.G Mecklenbrauker, *The Wigner Distribution - A Tool for Time-Frequency Signal Analysis, part 1: Continuous-Time Signals*, Phillips Journal of Research, vol. 35, no.3, pp. 217-250, 1980.
- [10] Goswami, Jaideva and Chan, Andrew. *Fundamentals of Wavelets, 1st Edition*, 301 pages, Wiley, Texas, 1999.
- [11] Alfredo Rosado Munoz, "Desarrollo de tecnicas de Deteccion de Fibrilacion Ventricular basadas en Algoritmos de tiempo-frecuencia." Las transformadas Tiempo-Frecuencia, Chapter 2.
- [12] L. Cohen, *Generalized Phase-Space Distribution Functions*, J. Math. Phys., vol. 7, pp. 781-786, 1966.
- [13] L. Cohen and H. Margeneau, *Probabilities in Quantum Mechanics, in Quantum Theory and Reality*, M. Bunge, Ed. (Springer, Berlin), chap. 4, pp. 71-89,

1967.

[14] Stark, H., ed. *Image Recovery: Theory and Application*. 1987, Academic Press:Orlando.

[15] Rick Trebino, et al., *Frequency-Resolved Optical Gating: The Measurement of Ultrashort Laser Pulses*. Kluwer Academic Publishers, Boston, chapter 8, 2000.

[16] Bracewell, R.N., *The Fourier Transform and Its Applications*. 2nd ed. 1986, New York:McGraw-Hill.

[17] Peatross, J. and A. Rundquist, *Temporal Decorrelation of short laser pulses*. Journal of the Optical Society of America B, 1998. 15(1):P. 216-22.

[18] Technology and Applications Center, Newport Corporation, *Application Note 33: Amplitude and Phase Characterization of Ultrashort Laser Pulses*.

[19] Julien Klein, Spectra-Physics: The Ti:Sapphire Laser, From Research to Industry and Beyond, [www.photonics.com/](http://www.photonics.com/), July 2010.

[20] Rick Trebino, et al., *Frequency-Resolved Optical Gating: The Measurement of Ultrashort Laser Pulses*. Kluwer Academic Publishers, Boston, chapter 6, p. 129, 2000.

# Appendix A

## Assembling FROG device

Actually, most of the steps followed in order to assembly a FROG device was explained in chapter 5. This appendix just pretends to give some guidelines and tips about how to build the FROG setup, trying to avoid systematic errors that could impair the pulse measurement.

I am not gonna waste time giving numbers about relatives distances between the optics placed in the setup, because some papers as *Application Note 33* from Newport company [18], listed above in *References*, do that.

I am just gonna give some pieces of advices, things that I have learnt from the practical experience in this work at the laboratory. There will have several generic tips about the work with optics and others more especific about the performing of a SHG FROG device.

1. The first thing that you have to realize yourself, is all the material you need. You need to know from the beggining if there are available all the items necessaries to assembly your setup. Maybe you note that you do not have all the items you need but may you have the possibility to make yourself a similar item with others you have availables at lab. It is so important in order to save time and money.
2. Once you have all the items/optics you need you have to check the power of your laser beam and the sensitivity of your detector/spectrometer and others, to avoid damaging any of them.
3. Working in the alignment of a laser beam could be a too hard, boring and at times, stressful task. So, my best advices are as follows:
  - (a) Be patient, spend enough time improving your alignment. An almost perfect alignment will make your next tasks easier.
  - (b) Don't get mad, crazy or anxious if your alignment is not perfect. Improve your alignment all you can, but not too much. If you cannot get

the second-harmonic beam at the end of the FROG setup, please, check the distances between the optics, the heights of the subassemblies where the mirrors, beamsplitters and others are placed with their respective mounts.

4. Check the bibliography that you have once and again, ask to your material company providers, maybe some optics have a wrong label in its box.
5. If your pulse length is 100 fs, please use a 100  $\mu\text{m}$  thickness BBO to generate your SHG signal.
6. Check the polarization of your beam at the entrance of your FROG device with a cube beamsplitter, maybe you need to change the polarization with a  $\frac{\lambda}{2}$  waveplate. If you have to use a waveplate, please use it between the beam and the FROG device. Don't place the waveplate into the FROG device.
7. Rotate the BBO mount until one of the SHG beam appear, from one of the two arms generated before into the FROG device. Then, go on rotating the BBO mount until the second SHG beam appear and then rotate the mirror at the middle point between the point where the other SHG beam appeared and where this last one did.
8. Use the dichroic filter to see clearly the SHG beam, a blue light, and not the red one. But after that, when you have found your middle point where your SHG FROG is placed, if the SHG pulse appears in the software too much attenuated, please, don't care about taking off the dichroic then, your iris assembly close to the spectrometer entrance will block the red beams contributions.
9. Build your FROG setup over a small table to be able of bringing your FROG to different locations in order to make different experiments.
10. Finally, make sure again the BBO mount is in the correct position, horizontally and vertically as well as the spectrometer input.

# Appendix B

## Dealing with Femtosoft and Newport softwares

### *Newport FROG Software*

It is a so important software, since with it we are gonna get the FROG trace from the minispectrometer. And after some problems and several modifications of the older version of the software, we decide to use the newest one, also making several changes in the code of the program. This work corresponded to our technical supporter from Newport.

So let's see some screenshots of the software and overe those pictures I am gonna comment a few important things to take in account.

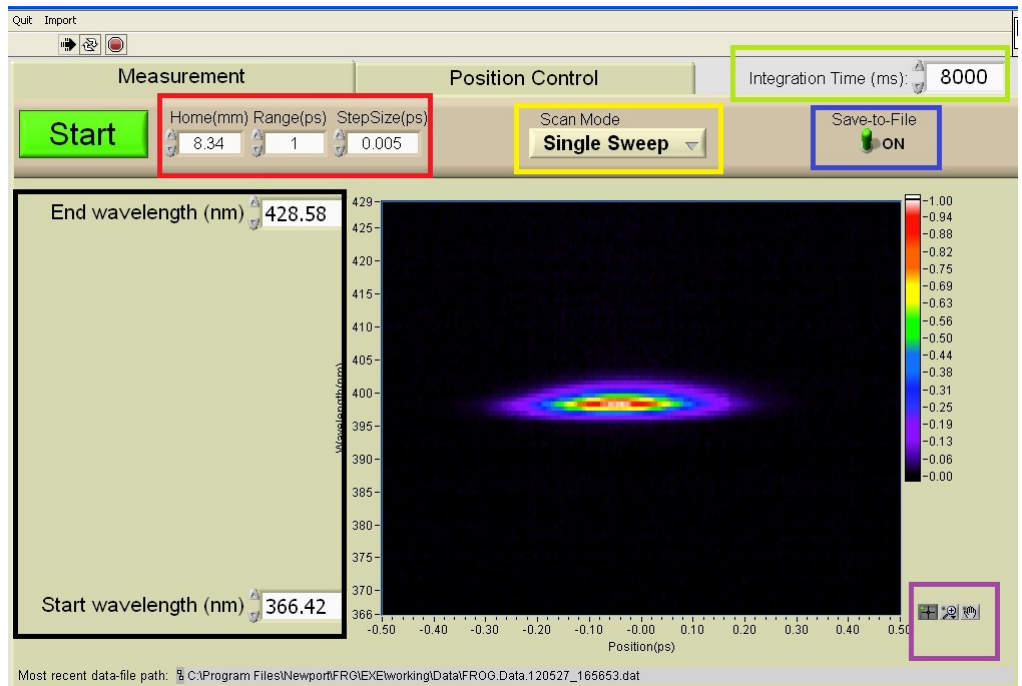


Figure 8.3: Newport FROG software Rev. 3

I have pointed with different colours boxes the parameters of the program to explain:

## RED BOX

HOME (mm): It's the home position where the delay line 2 is placed to see the SHG beam at the entrance of the spectrometer.

RANGE (ps): It's the range of the time delay axis of the graph in which are gonna see our pulse.

STEP SIZE (ps): This parameter determines the resolution of the measurement in time domain.

## YELLOW BOX

SCAN MODE: Offers two possibilities of scan, *Single Sweep* or *Non-stop Sweep*.

## GREEN BOX

INTEGRATION TIME (ms): This parameter permits us obtaining bigger or smaller amplitude of the SHG pulse received, and it's important to have a big enough amplitude to make our measurements properly. We have also to try don't saturate the spectrometer with a too high integration time.

## BLACK BOX

WAVELENGTH RANGE (nm): It determines the limits of the range of the wavelength axis.

## BLUE BOX

SAVE TO FILE: This button just save the trace measured or not, in a file into a path specified.

## PURPLE BOX

Those are some tools to manage the time-frequency graph representation.

## Femtosoft FROG 3.2.0 Software

The software of measuring seemed simple to manage, that is true. However, the software for analyzing the FROG traces obtained with the software before, it is not easy to manage at all.

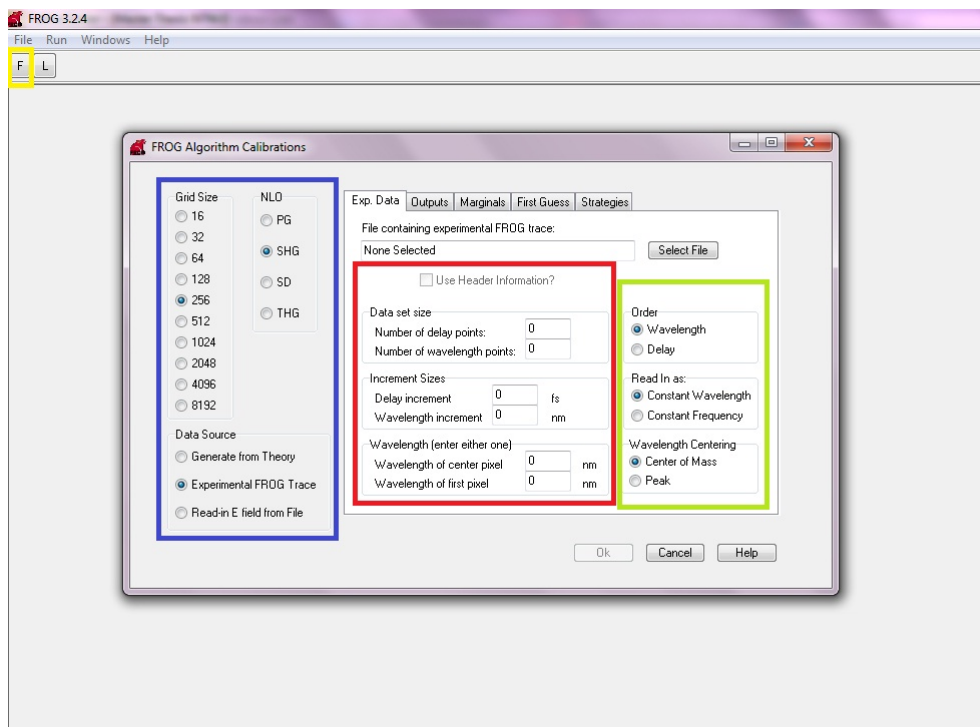


Figure 8.4: Femtosoft FROG 3.2.0 software

### YELLOW BOX

F: This button opens the window *Frog algorithm calibrations*, which permits us to manage the different aspects of the calibration of the FROG algorithm used in this analysis software, in order to get a more appropriate result from our FROG trace file obtained with the previous software.

### BLUE BOX

**GRID SIZE:** With this option we can choose the  $N \times N$  grid which will be used by the algorithm. Remember, the larger the grid size, the smaller the algorithm error but also the more computing cost.

NLO: This option permit us to choose the nonlinear effect of our trace.

DATA SOURCE: If the data to evaluate is theoretical or experimental. In our case, the second one.

## RED BOX

By marking the *Use header information*, is automatically load the features selected previously for the measuring software

## GREEN BOX

Some parameters to get a better graph representation and results.

The next window that appears is our trace.

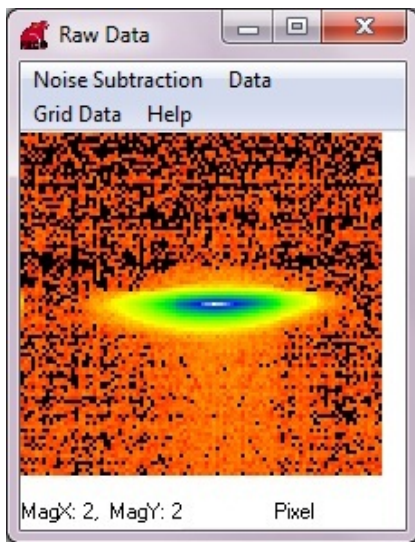


Figure 8.5: Raw Data

In order to get a better and cleaner trace before applying the algorithm we have some options to manage the trace representation, teh raw data:

Noise Subtraction: Permit us to eliminate the noise around the trace.

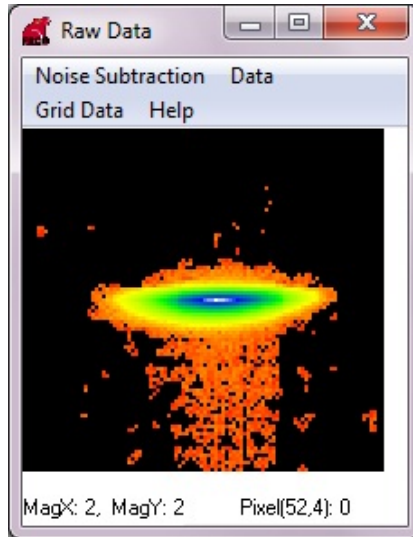


Figure 8.6: Noise Subtraction

Data: Permit us to extract roughly just the trace and also permit us to resample the time axis

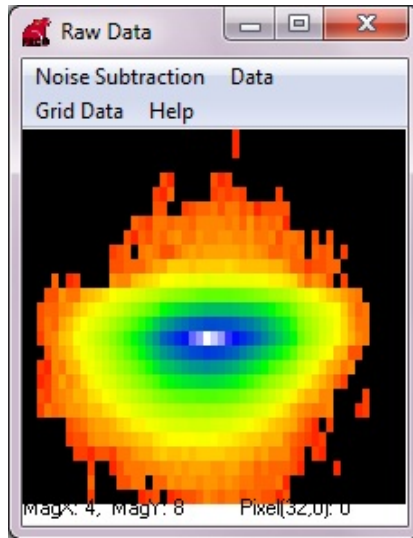


Figure 8.7: Data

After that, clicking on the option *Grid Data* we are gonna start to deal with the algorithm.

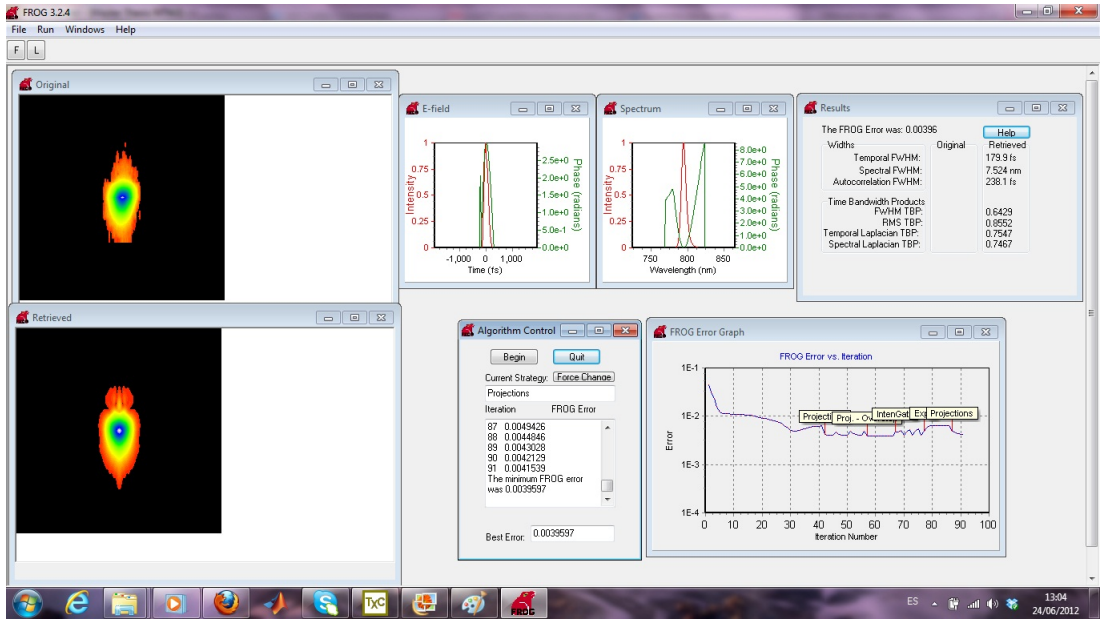


Figure 8.8: Algorithm running

We can run the algorithm clicking on the *Begin* button and then obtaining all the graphs and information about the original and retrieved pulse, the FROG error algorithm and the dispersive parameters of the pulse.

# Appendix C

## Matlab Code for plotting

This code is just for showing the graphs and traces generated mostly by FROG 3.2.0. from Femtosoft. Although is also shown one trace from the Newport's software, the most important, it is the FROG trace.

The script ShowFrog2012.m shows most of the figures that we have seen in measurements chapter. The script phases.m just show the last two graphs about both comparison the spectral phases and autocorrelations obtained in the different measures with the cuvettes filled with water.